Nanoscale Advances

ROYAL SOCIETY OF CHEMISTRY

REVIEW

View Article Online
View Journal | View Issue

Cite this: *Nanoscale Adv.*, 2024, **6**, 337

Effects of mechanical properties of carbon-based nanocomposites on scaffolds for tissue engineering applications: a comprehensive review

Reza Eivazzadeh-Keihan,*[a] Zahra Sadat,[a] Farnaz Lalebeigi,[a] Nooshin Naderi,[a] Leila Panahi,[a] Fatemeh Ganjali,[a] Sakineh Mahdian,[a] Zahra Saadatidizaji,[a] Mohammad Mahdavi,[b] Elham Chidar,[a] Erfan Soleimani,[a] Azadeh Ghaee,[c] Ali Maleki *[a] and Iman Zare *[d]

Mechanical properties, such as elasticity modulus, tensile strength, elongation, hardness, density, creep, toughness, brittleness, durability, stiffness, creep rupture, corrosion and wear, a low coefficient of thermal expansion, and fatigue limit, are some of the most important features of a biomaterial in tissue engineering applications. Furthermore, the scaffolds used in tissue engineering must exhibit mechanical and biological behaviour close to the target tissue. Thus, a variety of materials has been studied for enhancing the mechanical performance of composites. Carbon-based nanostructures, such as graphene oxide (GO), reduced graphene oxide (rGO), carbon nanotubes (CNTs), fibrous carbon nanostructures, and nanodiamonds (NDs), have shown great potential for this purpose. This is owing to their biocompatibility, high chemical and physical stability, ease of functionalization, and numerous surface functional groups with the capability to form covalent bonds and electrostatic interactions with other components in the composite, thus significantly enhancing their mechanical properties. Considering the outstanding capabilities of carbon nanostructures in enhancing the mechanical properties of biocomposites and increasing their applicability in tissue engineering and the lack of comprehensive studies on their biosafety and role in increasing the mechanical behaviour of scaffolds, a comprehensive review on carbon nanostructures is provided in this study.

Received 25th July 2023
Accepted 3rd December 2023

DOI: 10.1039/d3na00554b

rsc.li/nanoscale-advances

1. Introduction

Various types of composites have different features, including physical, chemical, mechanical, thermal, electrical, magnetic, acoustic, and optical. Among them, one of the most important features is their mechanical properties. For example, materials used in tissue engineering must exhibit similar mechanical behaviour to the target tissue.[1] The three general factors that determine the attributes of composite materials are as follows: (1) the constituent materials; (2) the geometric shapes of their constituent components, especially the reinforcing phase, together with the resulting structure of the materials; and (3) the interaction among the phases.[2]

Mechanical effects are physical properties that a material exhibits upon the application of a force. Examples of mechanical properties are elasticity modulus, tensile strength, elongation, hardness, density, creep, creep rupture, corrosion and wear, a low coefficient of thermal expansion (CTE), and fatigue limit. The mechanical properties of composite materials usually depend on their structure.[3] Composites are fabricated using various synthetic and natural materials, such as polymers,[4] hydrogels,[5] and nanomaterials (*e.g.*, nanocarbons).[6] Therefore, these properties usually depend on the shape of the inhomogeneities, the volume fraction occupied by the inhomogeneities, and the interfaces between the components.[3] In the new era of research, carbon nanostructures are one of the most important components for the preparation of composites, which is owing to their amazing mechanical characteristics.[7]

There are many different types of carbon nanostructures, such as graphene, graphene oxide (GO), reduced graphene oxide (rGO), carbon nanotubes (CNTs), carbon dots (CDs), carbon quantum dots (CQDs), nanodiamonds (NDs), carbon black, fullerenes, and carbon fibers (CFs).[8,9] These unique structures have been extensively studied in different biomedical applications, such as hyperthermia,[10] gene and drug delivery,[11] cancer therapy,[12] wound healing,[13,14] and tissue engineering.[15,16] The mechanical attributes of carbon nanostructures can originate from their physical properties or interactions with the other components in the composite.[17–19] These mechanical

[a]*Department of Chemistry, Catalysts and Organic Synthesis Research Laboratory, Iran University of Science and Technology, Tehran 16846-13114, Iran. E-mail: reza_eivazzadeh@alumni.iust.ac.ir; maleki@iust.ac.ir*

[b]*Endocrinology and Metabolism Research Center, Endocrinology and Metabolism Clinical Sciences Institute, Tehran University of Medical Sciences, Tehran, Iran*

[c]*Department of Life Science Engineering, Faculty of New Sciences and Technologies, University of Tehran, P.O. Box 14395-1561, Tehran, Iran*

[d]*Research and Development Department, Sina Medical Biochemistry Technologies Co. Ltd, Shiraz 7178795844, Iran. E-mail: imanzare146@gmail.com*

features usually affect the performance of the composite or its development (applications as absorbers, aerospace, marine, automotive, medical, construction infrastructure, and sports goods).[20] For example, the combination of GO with other components makes it a strong adsorbent for the absorption and desorption of *n*-hexane vapor, which is due to both to the enhanced specific surface area and micropore volume of the composite.[21] In the aerospace industry, CNTs have been used as a mechanical performance modifier due to their high specific surface area, mechanical strength, and inherent hardness.[22]

One of the most important applications of carbon structures is to the improve mechanical properties of materials in tissue engineering. In tissue engineering, despite the significant success achieved to date, tissue engineers face challenges in repairing or replacing tissues that principally have biomechanical functions. In tissue engineering, implanted cells, scaffolds, DNA, proteins, and/or protein fragments are used to repair, replace, and restore diseased or damaged tissue.[23,24] In this case, the ideal scaffold should not only have the same mechanical traits as the host tissue, but should also be able to degrade properly over time, preferably with a controlled rate of resorption, which ultimately creates a suitable space for new tissue growth.[25] Carbon nanomaterials have a large specific surface area, which makes them suitable for biomedical applications such as tissue engineering. Also, they show high drug loading and tissue loading capacities, together with good biocompatibility and long duration of action.[26]

Abundant evidence has shown that mechanical stress, together with other physical factors, may remarkably augment the biosynthetic activity of cells in biosynthetic matrices.[27,28] Although strength and work at failure both define the mechanical reliability of biomaterials, the elastic modulus is remarkably related to cellular material interactions. For example, the increase in Young's modulus can be calculated from the linear part of the stress–strain curve, which was used to analyze the stiffness of a cryogel after it was blended with CNTs in a compression test for skeletal card tissue engineering. This illustrated that the hardness of the cryogel significantly indicated the *in vivo* similarity of its mechanical properties at a hardness of 12 kPa.[29] Therefore, in general, it can be concluded that carbon structures increase the porosity, decrease the diameter, and accordingly cause increase the stability, Young's modulus, tensile strength, tensile modulus, tensile strength, compressive strength, compressive modulus, *etc.*[30,31] These properties of nanocarbons increase the resistance of scaffolds until complete regeneration of the tissue, and also create a space similar to the host tissue for the differentiation of the desired tissue.[32,33]

2. Biosafety of carbon nanomaterials: crucial for biomedical applications

The biosafety of nanocarbons is an important consideration for their biomedical applications. Although nanocarbons offer promising benefits, it is crucial to evaluate their potential risks and ensure appropriate safety measures are in place. Several aspects need to be considered regarding the biosafety of nanocarbons. For example, the potential toxicity of nanocarbons is a crucial aspect to address for their safe use in biomedical applications.[34] Their toxicity can vary depending on several factors, including the specific type of nanocarbon (*e.g.*, carbon nanotubes and graphene), dimensions (*e.g.*, length and diameter), surface characteristics (*e.g.*, functionalization and charge), and the biological system that they interact with.[35]

Some studies have indicated that certain forms of nanocarbon, particularly long and rigid carbon nanotubes, may induce inflammation or cellular damage under certain conditions.[36] However, it is important to note that extensive research has also demonstrated the biocompatibility and low toxicity of many nanocarbons when used at appropriate concentrations and properly functionalized.[37,38] Thorough toxicity assessments, including *in vitro* and *in vivo* studies, are necessary to understand the potential risks associated with specific nanocarbons and guide their safe application. Further, understanding the biodistribution and clearance pathways of nanocarbons is crucial for assessing their biosafety. Nanocarbons can be exposed to various routes in the body, such as systemic circulation, lymphatic drainage, and direct administration to specific sites. Thus, if nanocarbons persist in the body for extended periods or accumulate in specific organs, they can cause issues. Research has shown that the size, surface functionalization, and administration route can influence the biodistribution and clearance of nanocarbons.[39]

Nanocarbons, such as fullerenes, carbon nanotubes, graphene, and nanodiamonds, exhibit a remarkable array of attributes that distinguish them from conventional materials and make them highly attractive for a wide range of biomedical applications. One of the most intriguing aspects of nanocarbon materials is their unique structure and composition, which contribute to their exceptional virtues. For example, fullerenes are spherical carbon molecules with a hollow cage-like structure, while carbon nanotubes are cylindrical carbon structures. Graphene consists of a single layer of carbon atoms arranged in a two-dimensional honeycomb lattice, while nanodiamonds are diamond particles with nanoscale dimensions.[40]

These distinctive structures result in a plethora of desirable attributes, including high surface area, excellent mechanical strength, exceptional thermal and electrical conductivity, and outstanding optical properties, making nanocarbon materials powerful tools in various biomedical applications. For instance, their high surface area and unique electronic properties make them excellent candidates for sensing applications.[41]

The biological activity of carbon nanostructures highly depends on their type or functionalization. For instance, it was demonstrated that hydrophobic graphene shows a significantly higher cell proliferation rate than nanocrystalline diamonds.[42] Functionalized fullerenes have been reported to act as antioxidants in a variety of important biological applications. For example, polyhydroxylated fullerene, $C_{60}(OH)$, could prevent neuronal cell damage and death from radicals.[43] In a study by Zhang *et al.*, the observed that graphene at concentrations above 10 $\mu g\ mL^{-1}$ shows a time- and concentration-dependent decrease in metabolic activity.[44] In addition, the effect of GO

on human red blood cells has been studied. It was indicated that individual and small sheets of GO show greater hemolytic activity compared to its aggregated sheets. Interestingly, by improving the dispersion of GO with the aid of chitosan, its hemolytic activity was minimized and almost eliminated.[45] The cytotoxicity of CNTs limits their biomedical applications. However, their incorporation in hydrogel matrices, different functionalization, and size and dose alterations can severely alter their biocompatibility and solubility.[46] Functionalizing the hydrophobic surface of the CNTs, usually with carboxylic acid groups, improves their hydrophilicity and biocompatibility and endows them the ability to achieve targeted delivery.[47] In a study to determine the importance of the functionalization of CNTs on their cytotoxicity, phenyl-SO_3H and phenyl-SO_3 Na-functionalized SWCNTs exhibited no crucial mutilation on human dermal fibroblast cells even at high concentrations (>2 mg mL^{-1}), while SWCNTs functionalized with phenyl-$(COOH)_2$ manifested toxicity at low concentrations (80 μg mL^{-1}), which indicates the importance of functionalization on the toxicity of these materials. Also, by increasing the degree of sidewall functionalization, the SWCNT samples showed less cytotoxicity.[48] More examples of the different functionalization effects on carbon-based nanomaterials are provided throughout this manuscript.

Nanocarbon-based biosensors can detect specific molecules or biomarkers with high sensitivity, enabling the early diagnosis and monitoring of diseases. Additionally, their ability to interact with light at different wavelengths allows their use in advanced imaging techniques, such as fluorescence imaging and Raman spectroscopy, enabling the enhanced visualization of cells, tissues, and organs.[49] Nanocarbons also show great promise in the field of drug delivery. Their large surface area and unique chemical properties enable efficient loading and controlled release of therapeutic molecules, including drugs and genes. By functionalizing the surface of nanocarbons with targeting ligands, these nanomaterials can be specifically delivered to diseased cells or tissues, enhancing the treatment efficacy, while minimizing side effects. For instance, nanodiamonds have been extensively used in reinforcing biopolymers, resulting in the formation of biocomposites that can be applied in bone tissue engineering, chemotherapeutic drug delivery, and wound healing.[50] Besides, nanocarbon materials have shown great potential as photothermal agents for cancer therapy. Due to their exceptional light absorption and heat conversion activities, nanocarbons can be selectively heated upon exposure to near-infrared light. This localized heating effect can be harnessed for the targeted destruction of cancer cells, while minimizing damage to healthy tissues.[51]

In a study performed by Schrand and colleagues, it was reported that the biosafety of carbon-based nanomaterials is highly dependent on their type and concentration. In this study, different concentrations of NDs, CNTs, and carbon black (CB) were incubated with two different cell lines. The biocompatibility on both neuronal and lung cell lines followed the order of ND > CB > MWCNT > SWCNT. Apparently, NDs neither disturbed the macrophage mitochondrial membrane nor generated reactive oxygen species (ROS). In contrast, CNTs generated ROS and caused membrane leakage. Moreover, neuroblastoma cells lost their neurotic extension after being incubated with high concentrations of carbon nanomaterials.[52]

In summary, the advantage of nanocarbon materials is their biocompatibility, biodegradability, non-toxicity, and nonhemolytic nature, which are crucial for safe and effective biomedical applications. These properties reduce the risk of adverse reactions and allow their integration in biological systems without causing harm. Also, versatile functionalization of nanocarbon materials further expands their potential applications in biomedicine.

3. The role of mechanical properties of carbon-based nanomaterials in tissue engineering

The unique traits and applications of compounds are dependent on their physicochemical properties; therefore, the expression and measurement of these properties are considerable points in materials science. One of the most important physical features of compounds is their mechanical attributes, which define the behaviour of materials under the action of external forces.[53]

The mechanical properties of materials determine their strength, hardness, toughness, brittleness, durability, stiffness, and elasticity. The strength of a material refers to the amount of load that it can bear before fracturing or deforming, which is divided into several subcategories including tensile, compressive, shear, yield, and fatigue strength. Generally, the stress–strain curve is used to determine the strength and stiffness of materials.[54] The slope of the curve is called the Young's modulus and its value is typically large.[55] Many synthetic and natural compounds have significant mechanical features. Also, composites of these compounds possess high mechanical properties.

Composites are produced using two or more constituent materials, which have special activities compared to their components. To date, various composites have been synthesized, and due to their unprecedented mechanical and physical features, they have been widely used in different fields. Carbon composites are one of the principal types of composites and many studies have focused on their physicochemical properties and biological applications.[56,57] Carbon composites have high mechanical aspects due to the special structure of carbon-based nanomaterials and sp^2 hybridization carbon atoms. Mainly, carbon nanomaterials can increase the mechanical characteristic of composites due to the following reasons: (1) easy chemical functionalization,[58] (2) interaction of functional groups such as hydroxyl, carboxyl, ketone, and epoxy in various types of carbon nanomaterials with other functional groups in composite components,[59] (3) formation of strong π–π interaction between carbon sheets and other composite components,[60] and (4) formation of hydrogen bonding between the carboxyl and carbonyl groups of carbon nanomaterials and hydroxyl groups of other components in composites.[61]

According to the information provided in the literature, carbon nanostructures and the aforementioned interactions

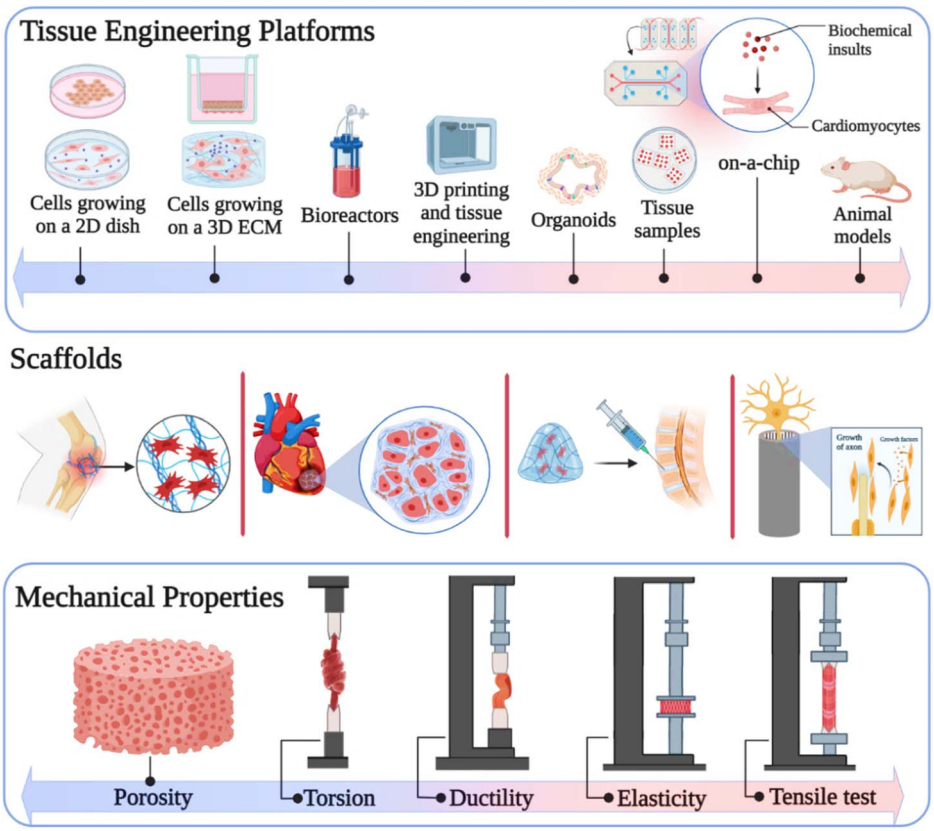

Fig. 1 Mechanical properties of carbon-based nanomaterials in tissue engineering. Created with ChemDraw and https://www.BioRender.com.

enhance the mechanical properties including compressive strength,[62] tensile strength,[63] toughness,[64] Young's modulus,[65] and elastic modulus[66] of composites. The effective mechanical properties of carbon nanomaterials in the composites facilitate their use in several biomedical applications, especially tissue engineering.[67] Carbon-based nanomaterials such as GO, CNTs, fullerenes, CDs, carbon diamond, CFs, and their derivatives improve the mechanical stability of scaffolds,[15] which play an important role in bone,[9] skin,[68] cartilage,[69] neural,[70] dental,[71] articular[72] and cardiac[73] tissue engineering. The scaffolds employed in tissue engineering must have appropriate porosity compared to the size of desired cells for promoting cell infiltration. Most compounds are utilized to increase the strength of composites, reduce the porosity, and ultimately decrease cell proliferation in tissue engineering. Alternatively, the advantages of carbon-based nanomaterials are that they do not limit the pore sizes of scaffolds in cell growth, while simultaneously enhancing their strength (Fig. 1).[74,75]

3.1. Graphene oxide and reduced graphene oxide

Go and rGO are members of the graphene family of carbon-based nanomaterials, which are synthesized using various methods. GO is the oxidized form of graphene, possessing hydroxyl, carboxylic, and epoxy functional groups, while rGO is a form of GO that has fewer oxygen molecules.[76,77] The particular physicochemical properties of GO and rGO such as mechanical strength,[78] large surface,[79] abundant functional groups,[80] and excellent hydrophilicity[81] make them suitable for application in the biomedical field such as drug delivery,[82] biosensing,[83] bioimaging,[84] cancer therapy,[85] tissue engineering,[86] and wound healing.[87]

Also, GO and rGO promote the biomechanical properties of composites by forming covalent, non-covalent, and electrostatic interactions in the composite structure. Therefore, numerous studies have been performed on the mechanical properties of GO and rGO and their effects on scaffolds employed in various types of tissue engineering. For instance, Fu *et al.* reported the synthesis of a polydopamine-assisted gold nanoparticle–poly(-lactide-*co*-glycolide)/L-lysine functionalized graphene oxide composite with mechanical strength, hydrophilicity, and antibacterial properties.[88] This scaffold could significantly promote new bone formation, which was based on L-lysine-functionalized GO and polydopamine-assisted gold nanoparticle coating PLGA scaffold material. The *in vivo* bone regeneration assessment exhibited the repair of a defect in the radius of rabbits after 12 weeks of treatment, while PLGA alone had a lower repair effect score. The GO in the scaffold improved the hydrophilicity, cell adhesion, compressive strength (2.68 ± 0.21 MPa), and elastic modulus (7.2 ± 1.47 MPa) of the composite. The synergistic effect of these properties makes it a good candidate for bone defect repair.

Studies have indicated the importance of considering the concentration of GO in biomedical applications.[89] For instance, in a study by Umar Aslam Khan and coworkers, by optimizing

the concentration of GO, the cell adhesion and proliferation were enhanced, while cytotoxicity was avoided.[90] Moreover, it was demonstrated that in the concentration range of 0.1–10 mg mL^{-1}, sulfonated GO is non-toxic and biosafe.[91] A recent study showed that 1.5 wt% of GO is the safest concentration for most cells, given that 3 wt% and 6 wt% exhibited significantly increased cytotoxicity on human bone marrow mesenchymal stem cells.[92] The swelling ratio of the hydrogels also varied after the addition of GO nanoparticles in their structure. It was demonstrated that by the addition of GO nanoparticles to a poly(acrylic acid) hydrogel, its deswelling ratio decreased, while the neat hydrogel swelled faster. These ratios were also found to be relevant to the content of GO.[93] The GO membrane and bulk GO swelling pressures were calculated in water and ethanol. It was demonstrated that under confinement conditions, the produced pressure could reach up to ~226 bar in water and 194 bar in ethanol. This significant swelling pressure is a key factor in applications that require GO membrane confinement or encapsulation.[94]

Another scaffold that is widely used in tissue engineering is polymeric scaffolds. However, a disadvantage of polymeric scaffolds is their low mechanical strength for tissue regeneration, and thus the use of other compounds such as GO is essential to upgrade their mechanical features.[95] Recently, Kadhim *et al.* reinforced polycaprolactone (PCL)–gelatin nanofiber scaffolds using bone morphogenetic protein (BMP)-modified GO.[96] In this case, although gelatin has favorable biological properties, it does not possess good mechanical stability, and therefore it was combined with PCL and GO to achieve the desired mechanical properties. Comparing the mechanical properties of gel/PCL and gel/PCL–GO–BMP (2.5 wt% GO) proved that the ultimate tensile strength increased from 8.5 ± 0.3 MPa to 17.2 ± 0.3 MPa, but the strain at break was reduced from 116% ± 6.2% to 90% ± 2.9% due to its high stiffness. Moreover, the swelling ratio increased significantly from 150% for gel/PCL to 218% for gel/PCL–GO–PAA*BMP. The interactions formed between the composite components determined the unique mechanical properties and applications of the scaffold in different tissue engineering. For instance, Shuai and colleagues fabricated HAp nanorods on a GO nanosheet *via* a *in situ* strategy for reinforcement of poly-L-lactic acid (PLLA).[97] The influence of the composite on cell growth and MG63 cell proliferation enabled its use in bone tissue engineering. The presence of abundant oxygen-containing groups in GO, which act as chelating sites, allowed HAp to be decorated on the GO in the form of nanorods. The special layer structure of HAp on the GO nanosheets induced the formation of chemical bonds between the composite and damaged bone. Specifically, 12% of GO–HAp increased the strength and modulus of the composite to 21.52 MPa and 4.99 GPa, respectively, through the formation of strong surface interactions with PLLA. One of the easy and appropriate strategies used in bone repairing is endogenous tissue engineering. In this method, hard cell culture is prevented and endogenous new stem cells are employed by implanting scaffolds. Therefore, Zhao *et al.* developed a bioinspired GO/chitosan/nHAP composite *via* a facile one-step *in situ* method for bone tissue engineering.[98] The *in vivo* cranium bone repair indicated that the defects were recovered to new tissue after 2–3 months of implantation. The electrostatic interaction between the amine groups of chitosan and carboxyl radical of GO enhances the mechanical features of the composite, and thus 0.99% of GO induced the highest compressive strength (0.124 ± 0.022 MPa) and elastic modulus (0.413 ± 0.213 MPa) in the scaffold. Also, the strong π–π interaction between the GO layers prevented the fracture of the composite by distributing the external stress

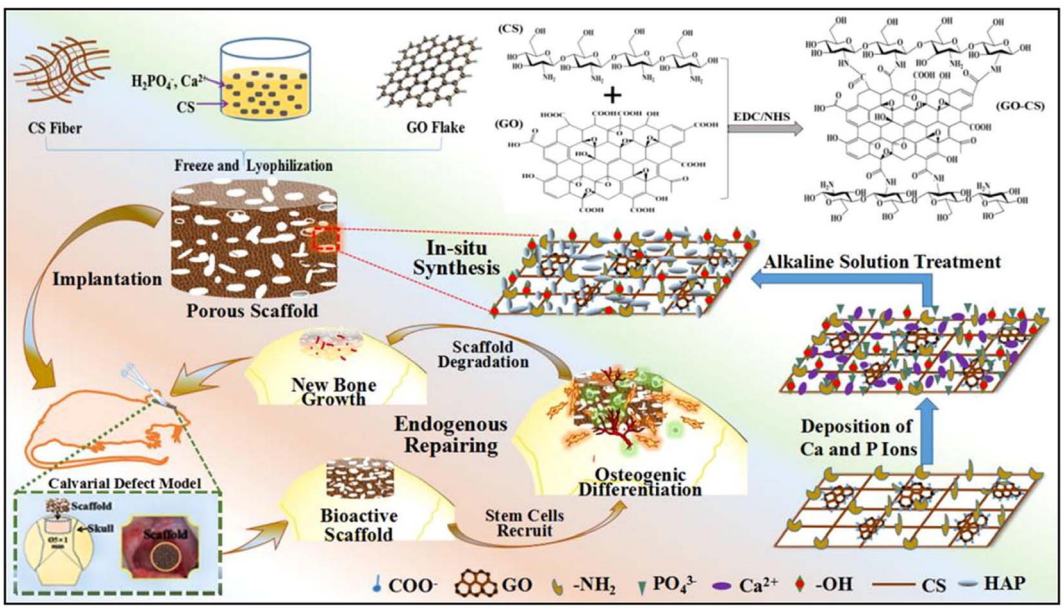

Fig. 2 Synthesis processes for GO/chitosan/nHAp scaffold and its implantation in a cranium bone defect in a rat. Reprinted with permission from ref. 98 Elsevier, copyright 2019.

between the GO sheets and the chitosan/nHAP matrix, and therefore it is efficient in engineering hard tissues. In addition, due to the higher hydrophilicity of GO/CS/nHAP, it was able to absorb more water than CS/nHAP, and therefore had a higher swelling ratio (Fig. 2).[98]

The main point in tissue engineering is that scaffolds should be similar to the extracellular matrix (ECM) of the target tissue in terms of physicochemical properties. Thus, Bahrami *et al.* synthesized collagen and rGO-coated collagen composite (rGO–Col) *via* chemical cross-linking and freeze-drying methods.[99] In this study, the regeneration of rabbit cranial defects after 12 weeks of implantation showed that rGO–Col can be used in implanting bone injuries. The addition of GO to the scaffold not only increased the proliferation of human bone marrow-derived mesenchymal stem cells (hBMSCs) but also compensated for the weak mechanical properties of collagen for bone structural support. According to the stress–strain curves from compression testing on Col–rGO and collagen, their elastic modulus was determined to be 325 ± 18 kPa and 115 ± 16 kPa, respectively, and thus the coated collagen with GO exhibited a 2.8-times increase in mechanical properties. Another challenge in tissue engineering, is articular cartilage regeneration. Accordingly, to repair this tissue, Gong and coworkers employed a natural acellular cartilage extracellular matrix (ACM) and cross-linked GO to ACM as a scaffold.[100] The function of GO is to improve the biomechanical strength of the composite and the ACM retains the ECM components such as type II collagen and glucosaminoglycan. *In vivo* implantation in a mouse knee joint exhibited that the defect area was completely repaired after 12 weeks of GO-modified 3D ACM implantation with traditional seed cells. Increasing the concentration of GO enhanced the elastic modulus (0.1518 ± 0.0067 MPa) and reduced the porosity of the composite, and thus the best scaffold contained 2 mg mL^{-1} of GO, which promoted cell adhesion and proliferation.

Another composite that has attracted significant attention in cartilage tissue engineering due to its structural similarity to GAGs found in the cartilage extracellular matrix is chitosan-based scaffolds. In 2019, Shamekhi *et al.* developed a chitosan-based composite that was reinforced with different concentrations of GO nanoparticles.[101] Increasing the mechanical properties of the scaffold by the addition of various amounts of GO prevented the scaffold from shrinking against the chondrocyte contraction and caused it to be completely placed on the defect side. The human articular chondrocyte culture on the scaffolds with different concentrations of GO exhibited that the enhancement in stiffness and modulus stimulated the proliferation of human articular chondrocytes. The stress–strain curves in this study demonstrated that an increase in the concentration of GO to 0.2% improved the Young's modulus, and therefore the use of compounds with high mechanical features such as GO is essential in cartilage tissue engineering.

One of the important mechanical characteristics determining the use of scaffolds in cartilage tissue engineering is their compressive strength. Cartilage tissue must have high compressive strength because it bears the weight of the body. In this regard, Nazar *et al.* reported the preparation of a gelatin hydrogel cross-linked with genipin and reinforced by GO-grafted chitosan.[102] The composite containing 0.06% w/w CS-*g*-GO possessed appropriate mechanical features such as Young's modulus (134.18 Pa), toughness (0.1235 J m^{-3}), and compressive stress (65 kPa). Also, the 90.2% viability of human chondrocyte cells, significant compressive stress, and high porosity (83.1 ± 2.6%) make this composite a favourable choice for cartilage repair. Interestingly, by increasing the CS-*g*-GO content, the swelling degree increased significantly from 800% to 1200%.

According to the ECM composition, density, and chondrocyte activity, cartilage is divided into different types, and thus repairing both superficial and deep parts of articular cartilage is noteworthy. In this case, Trucco and colleagues synthesized a bilayered hydrogel made of GO-doped gellan gum–poly(ethylene glycol) diacrylate with mechanical and lubrication features.[103] This hydrogel could be injected into chondral defects as a surgically implantable substitute and sequentially cross-linked by UV light and ionic cross-linking method. Doping GO in the hydrogel not only improved its lubrication properties and chondrogenic differentiation but also significantly enhanced the average fracture stress and toughness values from 194 ± 27 to 246 ± 34 kPa and 36 ± 3 to 41 ± 9 kPa, respectively. Due to energy distribution by the GO nanosheets, the increase in toughness indicated that the GO-doped hydrogel had better mechanical properties as artificial cartilage than the bare hydrogel. However, with the addition of the GO nanofillers, the swelling ratio of this composite slightly decreased with no statistical significance.

Another tissue that has attracted significant attention in tissue engineering owning to its low regenerative capacity is cardiac tissue. Many injectable hydrogels can be used in heart tissue engineering, but the noteworthy point is that the desired hydrogel should have sufficient resistance to the surrounding applied forces after injection at the infarct site. In this regard, Mousavi and colleagues developed oxidized alginate/myocardial ECM injectable hydrogels with electromechanical properties for cardiac tissue engineering. The addition of 3-(2-aminoethyl amino) propyltrimethoxysilane (APTMS)-functionalized rGO to the hydrogel improved its electromechanical properties.[104] The simultaneous increase in oxidized alginate from 3 to 4% w/v and 25 μg per mL rGO enhanced the Young's modulus from 22.1 kPa to 38.8 kPa. The Young's modulus of the native myocardium and cell viability of human umbilical vein endothelial cells indicate that this sample with an optimal concentration of rGO and oxidized alginate is a desirable hydrogel for cardiac tissue engineering.

One of the significant mechanical factors in heart pumping is the elastic property of the scaffold, which depends on the modulation of its failure. Thus, to investigate this mechanical feature, Nazari *et al.* incorporated two-dimensional nanomaterials, *i.e.*, MoS_2 and rGO nanosheets, in silk fibroin nanofibers *via* the electrospinning method for cardiac tissue engineering.[105] The *in vitro* assessment showed that the c-TnT and α-MHC levels as cardiac mature markers of TBX18-hiPSC cells increased by the SF/MoS_2 and SF/rGO composites. The

addition of rGO increased the mechanical properties of SF including Young's modulus (561 ± 8 kPa), yield strength (1.27 ± 0.04 MPa), ultimate strength (3.65 ± 0.05 MPa), and fracture modulation (103 ± 5). Therefore, it can be concluded that the elasticity feature of the desired composite should be similar to heart tissue. Another mechanical property of a scaffold that affects the contraction and expansion of the heart is the elongation at break. Recently, Azizi and colleagues developed polyurethane/rGO composite nanofibrous scaffolds with different microstructures for cardiac tissue engineering.[106] The rGO in the aligned scaffold increased the Young's modulus (496.4 kPa) and ultimate tensile strength (496.4 MPa) but decreased the elongation at break (52.07%) due to the small diameter of the fibers. The levels of troponin I as a cardiac gene indicated that the aligned composite enhanced the differentiation of satellite cells into cardiac prognostic cells. Consequently, to improve the efficiency of engineered tissue, all the mechanical properties of the tissue should be examined and

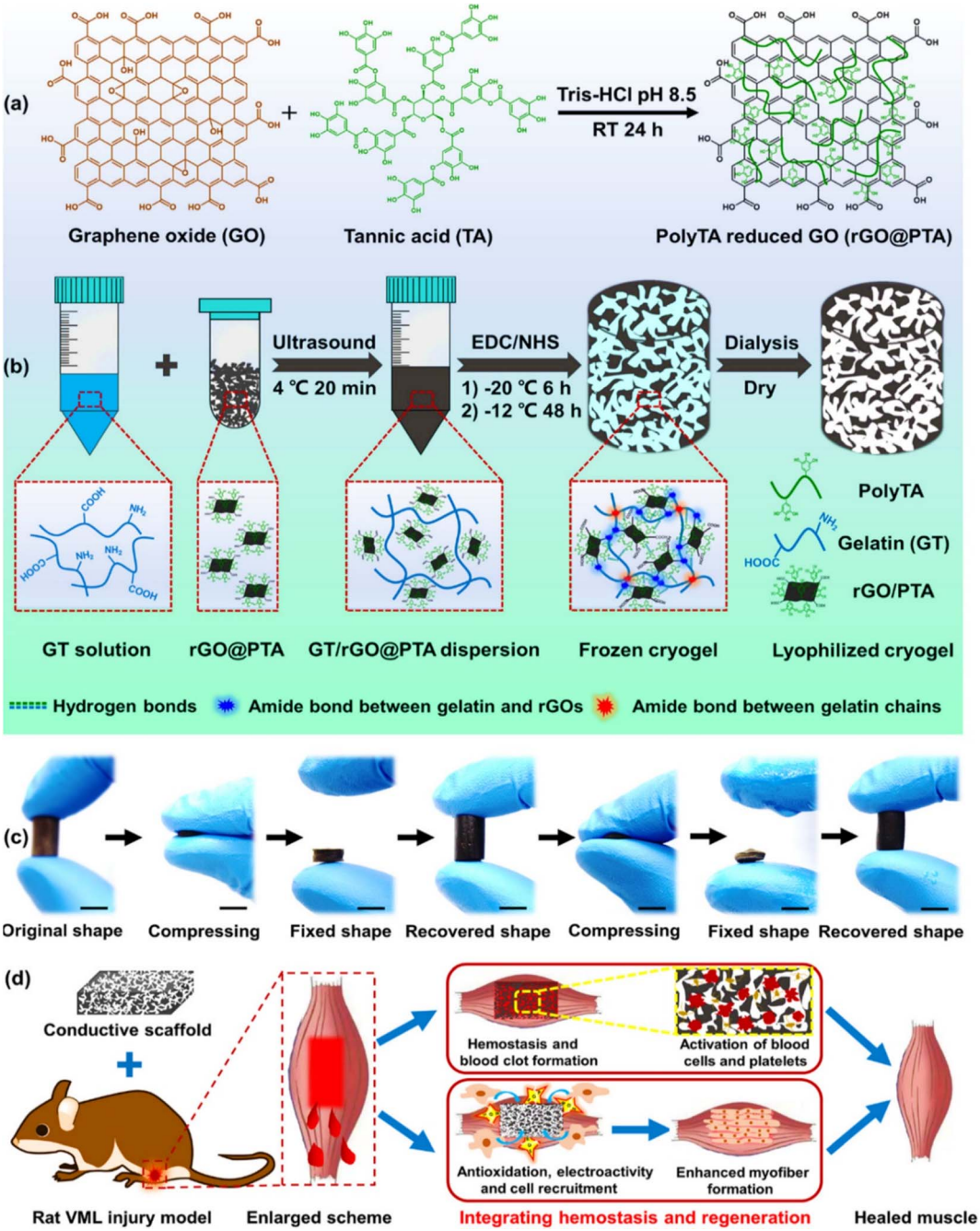

Fig. 3 An overview of the composite preparation, mechanical properties, and its application in skeletal muscle tissue engineering. (a) Synthesis of rGO–PTA, (b) synthesis and formation mechanism of the GT/rGO–PTA cryogel, (c) photograph of fixing and recovering performance of the cryogel in both dry and wet states (scale bar: 1 cm), and (d) schematic illustration of GT/rGO–PTA cryogel application in skeletal muscle repair by an *in situ* strategy. Reprinted with permission from ref. 107 Elsevier, copyright 2020.

a similar scaffold should be designed. Another serious muscle defect that affects movements is skeletal muscle defects. Recently, Zhao and coworkers designed a nanocomposite cryogel *via* the cryopolymerization of gelatin with poly(tannic acid)-reduced graphene oxide (rGO–PTA) for skeletal muscle tissue engineering. The 3D macroporous cryogel improved myogenic differentiation and C2C12 myoblast cells and also repaired volumetric muscle loss by integrating hemostasis. rGO/PTA as a cross-linked nanofiller in the composite network increased the compression modulus from 32 kPa to 75 kPa under 80% strain. In addition, the prepared cryogel could recover to its initial state after three compression–strain cycles due to its high elasticity and water adsorption. Thus, the presence of these excellent mechanical properties in the nanocomposite prevents the mechanical failure of the network (Fig. 3).[107]

Various occurrences such as accidents, bone fractures, trauma, and surgical complications lead to peripheral nerve damage, which may become long-term neurological disabilities, and thus artificial nerve guide conduits can be appropriate candidates for nerve regeneration. Recently, Abzan *et al.* developed a 3D polyvinylidene fluoride (PVDF)/GO scaffold *via* a non-solvent-induced phase separation method for nerve repairing.[108] The employed GO improved the piezoelectricity of the composite and enhanced its hydrophilicity and mechanical properties such as toughness (2.27 times) and strength (1.3 times) by the formation of strong interaction between fluorine groups and carbonyl groups (C=O) of GO nanosheets. These particular properties endowed to PVDF by 0.5 wt% GO led to the promoted attachment, spreading, and proliferation of PC12 cells, and also enabled it to act as a nerve conduit with 4 internal longitudinally aligned channels. Moreover, to have appropriate mechanical properties, the scaffolds used in nerve repair must also have high porosity and surface area to provide neurite length growth. In this regard, Jaswal and colleagues investigated an electrospun scaffold based on rGO-enfolded AuNPs integrated with PCL.[109] Due to the increased proliferation and differentiation of PC12 and S42 cells, this composite can be used for peripheral nerve regeneration. The integration of nanosized rGO converted the composite into an excellent neural conduit with unique electrical and mechanical properties, which had a large surface area. The mechanical tests indicated that the ultimate tensile strength of rGO-AuNPs–PCL is 5.8 MPa, while pure PCL had a low tensile strength (3.7 MPa). Consequently, the used rGO not only provides suitable mechanical properties for nerve tissue engineering but also increases the porosity of the composite for cell growth and transmission of electrical stimuli.

Nowadays, tissue engineering as an effective solution also plays a key role in cutaneous wound healing and burn treatment. For instance, You and coworkers designed a poly(lactic-*co*-glycolic acid) (PLGA) copolymer incorporating GO for skin tissue engineering.[110] According to the *in vivo* evaluations, the composite could enhance the skin wound healing rate in rats *via* exogenous electrical stimulation. The function of GO is to enhance the mechanical, electrical, and biological properties of the scaffold. The additional optimal concentration of GO (2%) increased the tensile strength (about 25 MPa) and surface roughness of the composite, improving the adhesion and proliferation of cells. In summary, the scaffolds based on GO and rGO nanomaterials play an important role in tissue engineering. The unparalleled mechanical strength, large specific surface area, abundant functional groups, and porosity of GO and rGO enable the use of different composites in various types of tissue regeneration. The mechanical properties of scaffolds are evaluated by different mechanical tests and these remarkable features provide appropriate conditions for cell growth, proliferation, adherence, and differentiation in various tissue repair including bone, cartilage, heart, nerve, and skin.

Table 1 summarizes the main characteristics and mechanical properties of GO and rGO composites proposed in the literature for tissue engineering.

3.2. Carbon nanotubes

CNTs are thin and long tubes consisting of a rolled-up graphene sheet having a diameter of about 100 nm. Carbon nanotubes can be mainly divided into 3 categories, *i.e.*, single-walled carbon nanotubes (SWNCTs), double-walled carbon nanotubes (DWNCTs), and multi-walled carbon nanotubes (MWNCTs). CNTs have attracted attention due to their phenomenal mechanical, thermal, and electrical properties.[9] Accordingly, CNTs and their related composites have been widely studied for tissue engineering applications.[160] The mechanical properties of carbon-based nanostructures have been of interest to scientists for a long time to strengthen the mechanical specification of composites or directly use these mechanical properties for their desired work. The mechanical effects of CNTs have been greatly noticed and used in applications such as medical,[161,162] pharmaceutical,[163] wound dressings,[164] various industries (namely aerospace, nano, and optics[165–168]), strengthening of electrical devices,[169,170] and tissue engineering.[27] In tissue engineering, the appearance of the materials used, which originate from their mechanical traits, plays an important role.

Based on previous studies, oriented CNTs exist in the form of sheets and yarns, which act as suitable substrates for the growth of various types of cells. For instance, the roughness and large exposed surface of CNTs may play an important role in their ability to favor neuronal adhesion.[171,172] In this regard, Li and coworkers designed and developed a nerve guidance conduit (including CNTs/sericin) with electrical conductivity, suitable mechanical features, and desirable swelling capacity for sciatic nerve repair. CNTs were added to strengthen the mechanical virtues of the composite nerve guidance conduit. The mechanical properties including tensile modulus (kPa), compressive modulus (kPa), tensile strength (kPa), compressive strength (kPa), and electrical conductivity (S cm^{-1}) with the addition of CNTs increased to 76.43 ± 11.01, 7.69 ± 0.59, 67.56 ± 2.47, 5.46 ± 0.88, $(3.90 \pm 0.26) \times 10^{-4}$, respectively. The porosity was also 85% with 0.5 mg per mL CNT, which is proportional to the optimal porosity for nerve regeneration (80%). The addition of these physical traits and improvement of mechanical properties by CNTs created an interconnected porous microstructure guiding channel for the axon longitudinal outgrowth exit and

Table 1 Mechanical properties of GO and rGO composites in tissue engineering

Composite	Type of tissue	Modulus	Strength	Porosity (%)	Optimum amount of GO/rGO	Cell viability (%)	Model(s)	Ref.
PU-GO/HAp	Bone	Young's modulus: 56.25 ± 2.19 MPa/ compressive modulus: 211.04 ± 12.94	Tensile strength: 13.25 ± 1.19 MPa/flexural strength 18.50 ± 0.07	85.8% ± 1.5%	2 wt%	~93%	*In vitro*	111
CO-*g*-GC-GO/AgNP	Skin	Young modulus: 2.19 ± 0.06 MPa/ compressive modulus: 5.21 ± 0.65 MPa	Tensile strength: 4.64 ± 1.40 MPa	59.29% ± 8.92%	Max 0.1 mg mL^{-1}	94.83 ± 4.95%	*In vitro*	112
HAP/ZrO_2/GO–PLA	Bone	Young's modulus: 0.211 ± 0.08 MPa	Tensile strength: 8.45 ± 1.1 MPa/fracture strength 0.43 ± 0.02	89.5% ± 2.5%	0.01 g	98.2 ± 5%	*In vitro*	113
ARX/GO/nHAp-NPs/ PVA	Bone	Young's modulus: 236.22 ± 3.80 MPa	Ultimate compressive strength: 7.94 ± 3.10 MPa	49.75% ± 3.10%	0.3 mg	98%	*In vitro*	114
PCL/rGO	Bone	Young's modulus: 20.11 ± 0.68 MPa	Ultimate tensile strength: 5.17 ± 0.95 MPa	87.79%	0.5 wt%	More than 100%	*In vitro*	115
HT-GO	Bone	Young's modulus: 71.77 ± 2.40 MPa	Compressive strength: 1.8 ± 016	89.7% ± 1.24%	1 wt%	More than 90%	*In vitro*	116
PCL-PU/SV-loaded GO	Bone	Tensile modulus: 29.80 MPa	Tensile strength: 70.87 MPa	N.A.	1.5 wt%	More than 85%	*In vitro*	117
CS-gel/GO/MMT	Bone	Young's modulus: 22.96 MPa	Compressive strength: 103.4 MPa	~90%	1 wt%	More than 80%	*In vitro*	118
BC-*g*-(Fe_3O_4/GO)	Bone	Young's modulus: ~200 MPa	Compressive strength: 11.66 MPa	48.79%	0.5 mg	More than 85%	*In vitro*	119
PLA/GO	Bone	Young's modulus: 2.6 GPa	Tensile strength 39 MPa	30%	0.3 wt%	N.A.	*In vitro*	120
SF/GO	Bone	Compressive modulus: 1.90 ± 0.084 MPa	Compression strength: 0.5 ± 0.052 MPa	71% ± 2.41%	10 wt%	OD value: about 1 (after 7 days)	*In vitro*	121
PCSG	Bone	Young's modulus: 72.4 ± 1.6 MPa	Tensile strength: 11.6 ± 0.5 MPa	88.1% ± 1.7%	2 wt%	N.A.	*In vitro*/*in vivo*	122
GG-AAc/GO/nHAp/ TiO_2	Bone	Young's modulus: 300.81 MPa	Compression strength: 13.31 MPa	44.32 ± 2.14%	0.3 mg	~85%	*In vitro*	123
DT/GO	Skin	Young's modulus: 10.18 ± 1.77 kPa	N.A.	51 ± 11%	3 wt%	~70% (after 7 days)	*In vitro*	124
PCL-Sr/Se-HAp/GO	Bone	Young's modulus: 5.34 ± 0.53 MPa	Tensile strength: 9.74 ± 0.43 MPa	47.7%	0.22 g	94.4% ± 3.1%	*In vitro*	125
SA–HA–GO	Bone	Elastic modulus: 149.4 ± 11.1 kPa	Compression stress: 165.5 ± 5.1 (60% strain)	77.08 ± 3.00	1.0 wt%	N.A.	*In vitro*/*in vivo*	126
CMCS/PVA	Skin	Young's modulus: 1.68 MPa	Tensile strength: 1.93 MPa	N.A.	5 wt%	88.6% ± 2%	*In vitro*	127
HA/gelatin/GO	Bone	Young's modulus: 397.11 ± 98.51 MPa	Compression strength: 10.28 ± 1.08 MPa Flexural strength: 12.58 ± 2.47 MPa	56.23 ± 1.07%	0.5% (w/v)	N.A.	*In vitro*	128

Table 1 (*Contd.*)

Composite	Type of tissue	Modulus	Strength	Porosity (%)	Optimum amount of GO/rGO	Cell viability (%)	Model(s)	Ref.
X/C/HAp/GO	Bone	N.A.	Compression strength: 0.9–1.1 MPa	90–93%	0.5–1 wt%	N.A.	*In vitro*	129
PASS/ZnO/GO	Skin	N.A.	Tensile strength: 2.34 MPa	N.A.	1 wt%	100% (after 7 days)	*In vitro*	130
SF/SPI/GO/β-TCP	Bone	N.A.	Compression strength: 0.802 ± 0.065 MPa	80.45 ± 2.04	10 mg	More than 100% (after 7 days)	*In vitro*	131
Gel-HA/VD-loaded GO	Bone	Young's modulus: 285.98 ± 90.2 MPa	N.A.	40.8 ± 7.1%	0.5 wt%	OD value: 0.16 (after 5 days)	*In vitro*	132
PB-GO	Cartilage	N.A.	Tensile strength: 2.08 ± 0.33 MPa	N.A.	1.5% (w/v)	108% ± 10.43% (after 7 days)	*In vitro*	133
HyA/gel/PEO-rGO	Skin	Young's modulus: 5176.62 MPa	Tensile strength: 108.53 MPa	N.A.	20 vol%	N.A.	*In vitro*	134
GO-CMC/PEGDA	Bone	Young's modulus: 11.02 ± 0.01 kPa	N.A.	87.4 ± 0.26%	0.1 mg L^{-1}	N.A.	*In vitro*/*in vivo*	135
Gelatin/GO/MgO	Bone	Tensile modulus: 1778.76 MPa	Tensile strength: 11.653 ± 1.23 MPa	N.A.	10 wt%	OD value: about 0.9 (after 7 days)	*In vitro*	136
np-HAp/GO/PEEK-p	Bone	Tensile modulus: ∼ 0.825 MPa	Tensile strength: 120 MPa	N.A.	1 wt%	OD value: more than 1 (after 7 days)	*In vitro*	137
SF/nHAp/GO	Bone	Elastic modulus: 279.73 kPa	Compression strength: 83.86 kPa	90.5 ± 1.1%	0.5 wt%	OD value: more than 1.2 (after 7 days)	*In vitro*	138
PLL-PLGA/GO	Bone	N.A.	Tensile strength: 9 : 65 ± 0 : 64 MPa	N.A.	2% (w/w)	N.A.	*In vitro*	139
RSF/rGO	Skin	Storage modulus: ∼ 18 kPa/ Young's modulus: ∼ 1.77 MPa	N.A.	N.A.	0.13 wt%	More than 86% (after 7 days)	*In vitro*	140
PCL/GO	Bone	Compressive modulus: 84.08 ± 3.93 MPa	Compression strength: 2.06 ± 0.11 MPa	N.A.	3 wt%	N.A.	*In vitro*	141
V-GO-gel	Intestinal	Young's modulus: 83.74 ± 4.37 MPa	Tensile strength: ∼ 5 MPa	N.A.	0.25% (w/v)	N.A.	*In vitro*/*in vivo*	142
PAmAA-Al^{3+}/PVA/GO	Skin	N.A.	Tensile strength: 370.7 kPa	N.A.	2 wt%	N.A.	*In vivo*	143
SMH/GO	Bone	Compressive modulus: 43 kPa	N.A.	N.A.	0.04 wt%		*In vitro*/*in vivo*	144
GO-CTS-CS	Skin	N.A.	Tensile strength: 10.10 MPa	N.A.	30 wt%	More than 90%	*In vitro*/*in vivo*	145
PVA/GRGO	Skin	N.A.	Tensile strength: 2.58 ± 0.43 Pa	N.A.	1.0 wt%	OD_{550}–OD_{600}: 0.4 (after 21 days)	*In vitro*	146
GelMA-PDA-rGO	Cardiac	Young's modulus: 23.6 ± 1.2 kPa	N.A.	N.A.	1 mg mL^{-1} with PDA	OD value: about 2 (after 5 days)	*In vitro*	147
SF–GO-PPY	Neural	Compressive modulus: 7.73 ± 1.22 kPa	Compressive strength: 530.89 ± 30.39 kPa	N.A.	5 mg mL^{-1} solution	N.A.	*In vitro*	148
RSF/GO	Nerve	Young's modulus: 122.7 ± 3.1 MPa	Breaking strength: 0.9 ± 0.1 MPa	N.A.	1.5 wt%	N.A.	*In vitro*	149
PVA/nano-HA/CTI/GO	Bone	N.A.	Tensile strength: 19.05 ± 0.03 MPa	N.A.	0.5 wt%	∼110% (after 5 days)	*In vitro*	150

Table 1 (*Contd.*)

Composite	Type of tissue	Modulus	Strength	Porosity (%)	Optimum amount of GO/rGO	Cell viability (%)	Model(s)	Ref.
PCL–GO/PHBV-$CaPO_4$	Bone	Elastic modulus: 52.21 MPa	Tensile strength: 2.87 MPa	N.A.	1 wt%	~110% (after 5 days)	*In vitro*	151
GelMA/GO	Neural	Storage modulus: 1.61 ± 0.06 kPa/ compressive modulus: 3.64 ± 0.43 kPa/ elastic modulus: 7.42 ± 0.29 kPa	N.A.	N.A.	1.40 mg mL^{-1}	~100%	*In vitro*	152
GO/ATP/COL	Bone	N.A.	Compressive modulus: 4.3 ± 0.5 MPa	56.0 ± 2.6%	0.5 wt%	N.A.	*In vitro*/*in vivo*	153
PVA/CS/GO-PEG	Skin	Tensile modulus: 2.42 ± 0.12 GPa	Tensile strength: 79.49 ± 3.97 MPa	N.A.	1 wt%	N.A.	*In vitro*	154
dECM–rGO	Cardiac	Compressive modulus: 17.5 ± 0.5 kPa	N.A.	N.A.	0.3% (w/v)	More than 90% (after 35 days)	*In vitro*	155
GH/GO	Skin	N.A.	Tensile strength: 53 kPa/adhesive strength: 73 kPa	N.A.	0.2 wt%	661% (after 7 days)	*In vitro*	156
Col–rGO	Cardiac	Young's modulus: 340 ± 20 kPa	N.A.	N.A.	400 μg mL^{-1}	OD value: ~0.7 (after 96 h)	*In vitro*	157
Gel/PCL–GO–PAA*(DCP)	Bone	N.A.	Ultimate tensile strength: 17.8 ± 0.2 MPa	N.A.	N.A.	N.A.	*In vitro*	158
ZnO/GO–CA	Skin	Young's modulus: 0.37 ± 0.18 MPa	Tensile strength: 8.82 ± 1.2 MPa	N.A.	0.5 g	97.38% ± 3.9%	*In vitro*	159

facilitated the exchange of nutrients and needed.[173] Nanofibrous nerve conduits manufactured with diverse synthetic and natural materials have enormous potential for back nerve regeneration as a bridge between adjoining ends. Interestingly, Wang and coworkers developed PLGA–MWCNT aligned nanofibers coated with poly-L-lysine for nerve tissue engineering. After the addition of MWCNTs, the scaffold possessed the improved mechanical properties of L-PC_A− and L-PC_A+, including ultimate tensile strength (MPa), elongation at break (%), and Young's modulus (MPa) of up to 2.92 ± 0.12, 127.81 ± 2.92 and 6.82, 58.03 ± 2.94 and 22.47 ± 1.36, 31.96 ± 8.65, 485.05 ± 49.55, respectively. Consequently, the scaffold could guide PC12 cells and grow DRG neurons along the fiber direction, which is beneficial for neurite outgrowth, making it a potential candidate for nerve regeneration in tissue engineering.[174]

Biocompatible scaffolds in tissue engineering offer an appropriate micro-environment for the regeneration of injured tissue and the attachment and growth of cells. CNTs, as promising materials, can create a similar micro environment for bone repair in osteonecrosis and the natural function of bone and cartilage such as mechanical strength.[175] In another study, Shuai *et al.*, after bonding 3D hybrid montmorillonite (MMT)/CNT (MMT–CNT) with an optimal weight ratio of MMT : CNT 1 : 0.1, and embedding it in PLLA by the SLS method, prepared a self-assembly scaffold. The addition of CNTs, besides reducing the accumulation of MMT by being sandwiched between its middle layer, increased the mechanical effects of the scaffold due to the tolerance of the stress transferred from the matrix, which was high due to their high strength and modulus and large specific surface area. Adequate mechanical traits are essential during the induction of bone scaffolds. The results of the mechanical tests (tensile strength and modulus 113.04% and 111.46% and compressive strength and modulus 58.20% and 63.27%, respectively) showed that the addition of CNTs to the scaffold structure in this bone tissue engineering further facilitated the transfer of nutrients due to the uniform distribution of pores on the scaffold and its rapid degradation created space for the growth of bone tissue.[176] Because of their special mechanical properties, CNTs can act as an interface for strong interfacial bonding and increased adhesion. In this respect, hydroxyapatite–carbon nanotube–wood derived carbon (HA–CNTs–WDC) composites have been developed as scaffolds for bone engineering by electrochemical deposition and chemical vapor deposition methods. The CNTs present in the structure, in addition to promoting HA/WDC interfacial adhesion, with their porous structure, increased the HA nucleation points and uniformity, and consequently increased the mechanical attributes of the scaffold. The improvement in mechanical properties with the addition of CNTs was proven by the increase in the values of compressive strength (10.54 MPa) and compressive stress (almost 12 MPa).[177]

The biocompatibility of the composites based on CNTs is highly dependent on the concentration of these nanoparticles in the composite. Sang *et al.* proved that by increasing the MWCNT concentration in a composite from 1% to 5%, its cytotoxicity increased. Also, by increasing the MWCNT concentration, the swelling ratio decreased.[178] Other studies also indicated the biocompatibility of the CNTs at low and controlled concentrations.[179] Besides concentration, the size and shape of CNTs play a decisive in the biocompatibility of the composite and are related to cell damage and cell destruction.[52]

The incorporation of CNTs in the hydrogel matrix can effectively increase its swelling capacity. In the study by Tong and coworkers, it was indicated that by adding CNTs to a polyvinyl alcohol (PVA) hydrogel matrix, the swelling properties were enhanced as well as the tensile modulus, tensile strength, and strain at break. The final swelling ratios increased by 35.7% and 44.9% at room temperature and 310 K, respectively.[180] As another important aspect of materials used in tissue engineering, the biodegradation of CNTs has been studied. For example, Zhang and coworkers investigated the relationship between the physicochemical properties of CNTs and biodegradation. It is believed that the key oxidizer of CNTs in macrophages is sodium hypochlorite. Therefore, it was used for investigating the biodegradation of CNTs. It was indicated that the biodegradation of CNTs is generally related to their diameter and degradation followed the order of SWCNT ≥ carbon nanohorns > thinner MWCNT ≥ thicker MWCNTs.[181]

In terms of structural–chemical, biological, and mechanical properties, MWCNTs simulate the ECM and participate in bone regeneration as a composite reinforcing material. In the designed and developed scaffold of dendrimer-MWCNT reinforced SrHAP composite, the presence of MWCNTs resulted in: (1) 30-fold increase in curcumin loading, (2) 1.7-fold delay in its burst release, (3) creation of porosity of 89.63% ± 2.4% in the composite, which is comparable to human cortical bone, (4) creating mechanical strength of 0.415 ± 0.04 GPa, (5) guiding bone repair due to homology and 3D structure similar to spiral collagen, and (6) a pattern for apatite nucleation due to anionic chemical properties in nanotubes. Thus, due to all these reasons, especially in creating the appropriate mechanical features, the differentiation of MG-63 human bone-like cells improved and increased.[182]

In the report by Kaur *et al.*, the addition of COOH-SWCNTs to the CS-Coll/COOH-SWCNTs composite changed the structural morphology of the hydrogel into a parallel network with a porosity of 88% ± 3%. In addition, it has caused a 63% increase in mechanical properties (storage modulus (almost 110 Pa), loss modulus (around 5 Pa), and Young's modulus (around 106–107 Pa)), which increased the mechanical strength of the hydrogel from kPa to MPa, making it closer to the mechanical strength of bone. Thus, the composite was proven to be suitable as an injectable scaffold capable of cell differentiation and proliferation. The swelling ratio and degradation rate were found to be dependent on the composition with the optimal PBS absorbance through Fickian diffusion and stability in a liquid environment.[19] In another study, they prepared a scaffold that included PCL membranes, β-glycerol phosphate (β-GP), and functionalized multiwall carbon nanotubes (f-MWCNTs), which provided a potential alternative for bone tissue regeneration with viability and proliferation of HDPSCs *in vitro*. The addition of f-MWCNTs increased the Young's modulus and the maximum tensile strength to 405.9 MPa and 25, respectively, which greatly contributed to the production of

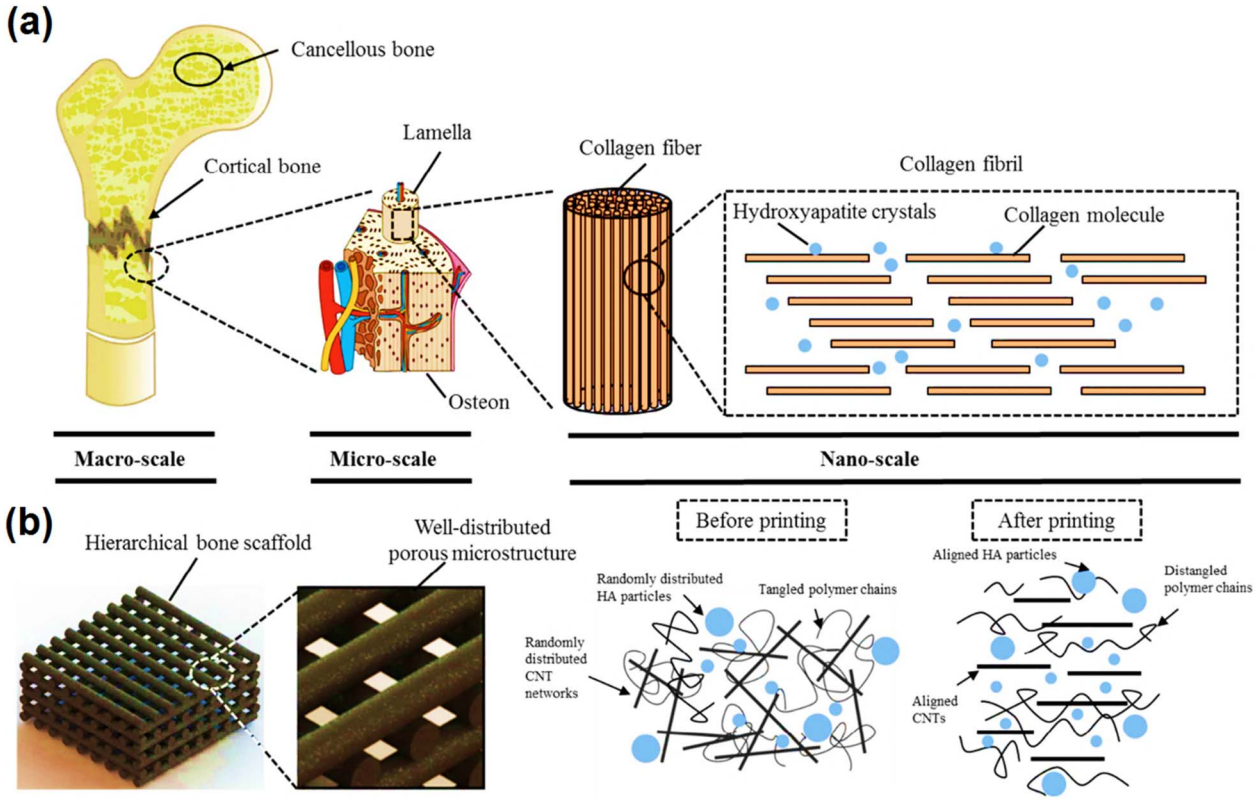

Fig. 4 Schematic of the hierarchical scaffold system with uniform geometry at the microscale and highly aligned structures at the nanoscale that mimics the bone structure from the macroscale to the nanoscale (a and b). Reprinted with permission from ref. 184 Elsevier, copyright 2020.

a highly efficient bone biomaterial with the ability to release bioactive factors and stimulate bone formation.[183]

The purpose of tissue engineering is to repair, replace, and restore unhealthy or damaged tissues, where the mechanical properties of scaffolds, especially the ability to mimic natural tissue, are significant. In bone tissue engineering, the ECM consists of collagen and inorganic bone minerals, which are hierarchically organized on multiple-length scales. In this direction, in an investigation, a highly biomimetic 3D printed porous scaffold comprised of MWCNTs with the same dimensions as collagen fibers, which were mainly aligned along the printing direction, was coupled with nHA and blended with a PCL matrix to produce scaffolds using a production system based on extrusion with the help of screws. Also, besides increasing the storage modulus, the elastic modulus of the filament (compressive modulus was almost 90 MPa) and the yield strength (almost 3 MPa) of the scaffold, the surface roughness increased, which promoted bone differentiation, helped to adjust the path of the hard surface transfer mechanism and enabled high protein absorption (Fig. 4).[184]

Tissue engineering is a promising method to regenerate damaged tissue by inducing the ability of natural tissue to heal using a cell scaffold that is transplanted into the host tissue. For example, Miyanji *et al.* designed and synthesized chitosan–gelatin/single-walled carbon nanotube electrospun composite scaffolds for cartilage tissue engineering, which is a connective tissue with a slow healing rate. CNTs functionalized with COOH provide interaction between themselves and biopolymers, which leads to better interface bonding and improved mechanical specs. Thus, their addition as a polymer matrix reinforcement due to their special properties, including high inherent mechanical properties, reduced the fiber diameter, contact angle, and elongation at break (3.26% ± 0.02%), and also increased the tensile strength (3.26 ± 0.02 MPa), Young's modulus (187.56 ± 9.31 MPa) and hydrophilicity of the scaffold, which enhanced the stability, cell viability, and cell behaviour to repair cartilage tissue to absorb growth factor. Their tubular structure allows them to transfer the external load from the matrix (the outermost layer) to the inner layers as a bridge in the polymer matrix. In addition, they create a porosity of over 80% (necessary for tissue engineering) in the scaffold, which plays an important role in the penetration of oxygen, humidity, and the transfer of nutrients to the cells and the removal of waste materials from them.[185]

Synthetic materials that are used for bone grafting in fracture must be attached to the porous bone, and thus the synthesized scaffold, besides biodegradability, must have sufficient compressive strength that is more than 2 MPa. For example, Akbari-Aghdam and coworkers fabricated a scaffold of polymer nanoceramic materials with controlled porosity that is similar to cancellous bone tissue and includes components such as resin polymer, SWCNT, and hydroxyapatite (HA) made by the digital light processing method. SWCNT having a suitable porosity of nearly 55% made the scaffold similar to the

porosity of human bone, with acceptable strength. It also increased the mechanical properties of the sample up to 36 MPa and increased protein conversion and absorption in human bone.[186]

In skeletal muscle tissue engineering, the engineered scaffold must have the ability to endure periodic contractions and rest in daily life, which, in addition to having the same structure as the original tissue, requires excellent mechanical features to withstand continuous movements. Skeletal muscle tissue has compressive properties and a regular structure that is sensitive to electrical signals. Alternatively, platforms using biomimetic 3D aligned conductive tubular cryogel scaffolds consisting of gelatin and polydopamine-coated carbon nanotubes (PCNTs) by unidirectional casting technology by anisotropic compression as a framework, with a parallel structure were developed for 3D cell alignment and differentiation of C2C12 myoblasts and skeletal muscle regeneration *in vivo* in a rat tibialis anterior muscle defect model. The combined CNTs not only increased the conductivity, but also enhanced the mechanical attributes of the cryogel, including the compressive modulus in the longitudinal section to 66.3 ± 9.42 kPa, enabling the cryogel able to withstand repeated contraction behaviour and dynamic contraction similar to native skeletal muscle (Fig. 5).[187] In a report on the design of scaffolds for use in heart and nerve tissue engineering, a CNT/PCL/gelatin composite was prepared by "sandwich" (sCNT) and dual deposition (DD CNT) methods. According to the report, the presence of CNTs, in addition to increasing the fiber diameter, pore size, and hydrophobicity of the scaffold, electrical conductivity up to 5.22 ± 0.49 kS, 80% increase in Young's modulus and 28% in tensile strength, and decrease in the rate of degradation, the scaffold also showed antimicrobial activity. Consequently, cell migration into the scaffold was promoted, making it a potential scaffold for the differentiation of heart and nerve cells (spinal cord and neural growth substrate).[188]

Cardiovascular tissue is exposed to continuous pulsating flow and mechanical stress, and blood vessels always faces pulsating shear stress of blood flow. Therefore, in cardiovascular tissue engineering, Tondnevis *et al.* prepared a scaffold consisting of gelatin, SWCNT, and polyurethane fiber. The addition of SWCNT increased the Young's modulus and ultimate strength of the scaffolds up to 16.47 ± 0.5 and 23.73 ± 0.5 MPa, respectively, reduced the average diameter to 140 nm, increasing the porosity to 89% ± 5% and hydrophilicity, and improved and increased the mechanical properties of the scaffold for it to withstand the above-mentioned physiological conditions. Studies indicated that the incorporation of CWCNTs in the composite structure reduced the degradation rate of the samples. The Young's modulus and ultimate stress were comparable to native myocardium tissue due to the strengthening effect of SWCNTs.[189] In another study, a three-layer hybrid nanobiocomposite based on ultrahigh-molecular-

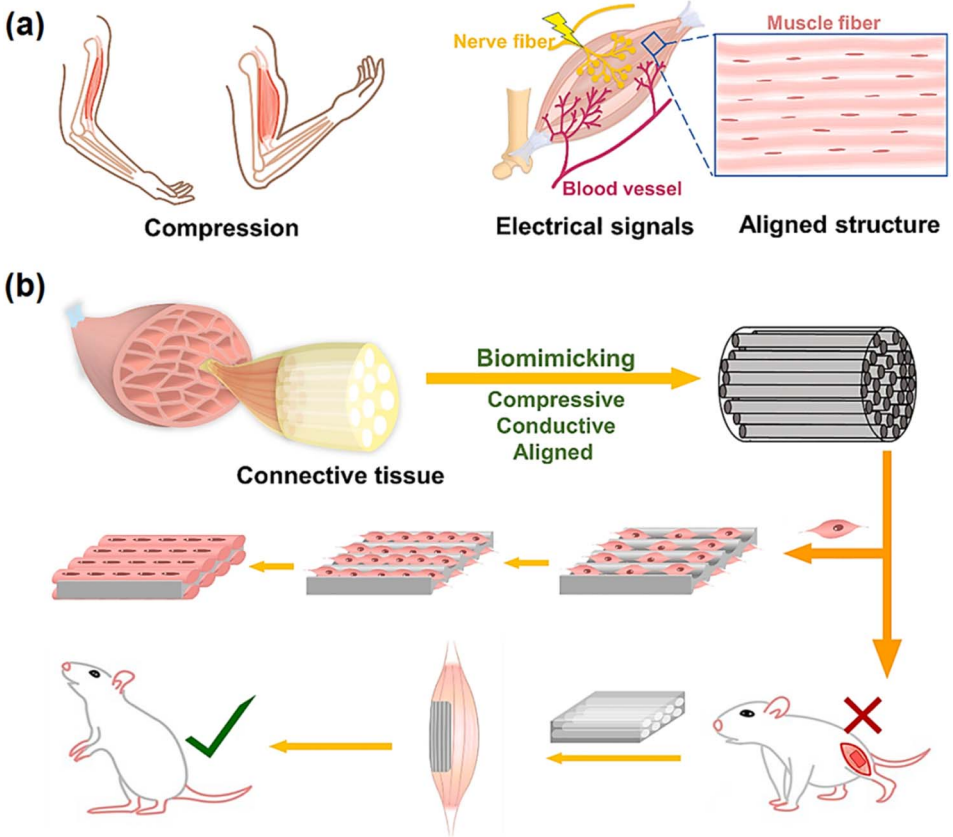

Fig. 5 (a) Properties of skeletal muscle tissue. (b) Schematic of the process of using a gelatin cryogel scaffold based on a PCNT in desired skeletal muscle tissue engineering. Reprinted with permission from ref. 187 Elsevier, copyright 2022.

Table 2 Mechanical properties of CNT composites in tissue engineering

Composite structure	Type of tissue	Modulus	Strength	Porosity, %	Optimum amount of CNTs	Cell viability, %	Model(s)	Ref.
ACNTs-doped PMMA composites	Bone	Elastic modulus: almost 175 GPa	Compressive strength: almost 130 MPa	N.A.	6 wt%	N.A.	*In vitro*	195
COL/MWNT composite film	Nerve tissue	Young's modulus: almost 5 MPa	Tensile stress–strain curves: almost 40 MPa-8%	N.A.	0.15%	Almost 80	*In vitro*	196
CNT-reinforced PCL	Non-soft tissues (*e.g.*, cartilage, tendons, and meniscus)	Elastic modulus: almost 1200 MPa	N.A.	N.A.	0.01%	95%	*In vitro*	194
PHB-Cs/MWCNTs coating deposited on nBG/nTiO	Bone	Compressive modulus: 0.33 ± 0.004 MPa	Compressive strength: 11.14 MPa	79.08 ± 0.8	1 wt%	OD: around 2.5	*In vitro*	197
PLGA/SiO_2NT nanocomposite	Bone	Young's modulus: around 64.15 GPa, shear modulus, *G* and bulk modulus, *B*: around 0.0000 GPa	N.A.	N.A.	N.A.	N.A.	*In vitro*	198
HA/HDPE/MWCNT bio-composites	Bone	N.A.	Tensile strength: 135.56 MPa	N.A.	1%	N.A.	*In vitro*	199
HA–alginate–SWCNT composite	Bone	Young's modulus *E*: 0.645 ± 0.028 GPa	Compressive strength σ_c: 202 ± 9 MPa	N.A.	0.5%	N.A.	*In vitro*	200
SWNT-COOH/Coll	Cartilage	N.A.	Compressive strength: almost 14 kPa	N.A.	0.5 wt%	N.A.	*In vivo*	28
PAAm/SA/CNTs/$CaCl_2$ hybrid DN hydrogels	N.A.	Young's modulus: 9.16 kPa	Tensile strength: 271.68 ± 6.04 kPa, compressive strength: 801.95 ± 284.63 kPa, compressive strain: 763.39% ± 45.42%	Almost 70	0.5 wt%	N.A.	N.A.	201
PCL/MWCNT	Bone	Compressive modulus: almost 80 MPa	N.A.	N.A.	3 wt%	N.A.	*In vitro*	202
HA-CNT nanofibers	Nerve tissue	Bulk modulus: 1.769 ± 0.26, local modulus: 174.85 ± 31.9 kPa	Strength: 0.583 ± 0.08 MPa	N.A.	0.01%	N.A.	*In vitro*	203
AG-Col-*o*-CNT scaffolds	Bone	Tensile modulus: almost 240 kPa	N.A.	N.A.	200 mg	N.A.	*In vivo*	204
CS/PVA/CS-*g*-CNO nanocomposite films	Bone	Young's modulus: 2.26 ± 0.15 GPa	Tensile strength: 28.0 ± 2.27 MPa	N.A.	500 mg Cl–CNO	N.A.	*In vivo*	205
c.p.Ti-CNT nanocomposite	Bone	Young's modulus: 7.19 GPa ± 0.40 GPa, elastic modulus: 112.3 GPa ± 3.7 GPa	N.A.	1.29 ± 0.83 μm^2	5%	90%	*In vitro*	206
P3HB-chitosan-MWNTs/silk nano-micro-scaffold	Cartilage	N.A.	Ultimate tensile strength (mean ± SD): 46.68 ± 2.20 MPa, ultimate tensile strain (mean ± SD): 33.19% ± 1.18%	83.78	1 wt%	N.A.	*In vitro*	207

Table 2 (*Contd.*)

Composite structure	Type of tissue	Modulus	Strength	Porosity, %	Optimum amount of CNTs	Cell viability, %	Model(s)	Ref.
PEDOT/CNT scaffolds	C8-astrocytes	Young's modulus: almost 60 kPa	N.A.	Almost 60 (pore size mostly 50–100 μm)	30%	N.A.	*In vitro*	208
N.A.	Hard tissue	N.A.	Tensile strength: around 10 MPa	83	0.5%	N.A.	*In vitro*	209
Gel/Akr/Fe_3O_4/MWNT	Bone	Elastic modulus: 0.45 ± 0.1 GPa	Compressive strength: 3.82 ± 0.2 MPa	76 ± 3	10% w/w	Around 90	*In vitro*	210
CMX-*g*-PAA/Fe^{3+}/HCNTs hydrogel	N.A.	N.A.	Compressive strength: 10.4 MPa	N.A.	0.15	N.A.	*In vitro*	211
MWCNT-containing PCL-based scaffold	Cartilage	N.A.	Tensile strength: around 2.4 MPa	Around 75	10%	Around 120	*In vitro*	212
ALG *in situ* gel-forming PLGA–CNT microspheres	Nerve	Loss modulus: 10^3 Pa	N.A.	N.A.	10%	70%	*In vitro*	213
PCL/CNT scaffolds	Bone	Compressive modulus: 45.47 ± 1.12 MPa	Compressive strength: 3.83 ± 0.28 MPa	N.A.	3 wt%	Fluorescence intensity around 5800	*In vitro*	214
PU/silk-fMWCNTs scaffold	Nerve tissue	N.A.	Tensile stress: ~16.21 MPa	N.A.	3 wt%	N.A.	*In vitro*	215
CNT-TES-PAMAM-G3-collagen scaffolds	Bone	Young's modulus: 369.62 ± 5.2 MPa	Tensile strength: 17.15 ± 1.7 MPa	96	100 mg	Around 90	*In vivo*	68
PLA/PCL/MWCNTs nanocomposites	N.A.	Modulus: 2.81 ± 1.00 GPa	N.A.	N.A.	0.5%	N.A.	N.A.	216
PNIPAM/L/CNT hydrogel	Human motion sensing	Modulus: 46.8 kPa	Adhesive strength: almost 7 kPa, tensile stress: 0.53 ± 0.02	N.A.	4 mg	N.A.	*In vitro*	217
CS/PVA/ox-CNO biodegradable scaffold	Skin	Young's modulus: 3.86 ± 0.77 GPa	N.A.	N.A.	1%	N.A.	*In vivo*	218
MWCNTS/BG/PEEK	Bone	Tensile modulus: 6.1 GPa	Tensile strength: 93 MPa, bending strength: 170 MPa	N.A.	4%	OD: 0.7	*In vitro*	219
Ag/MWCNTs	N.A.	Elastic moduli: around 1030 G' and viscous moduli: around 130 G''	N.A.	N.A.	20 mg	N.A.	*In vitro*	220
PCL/PEG/MWCNT	Myocardial tissue	Elastic modulus: almost 55 MPa	Tensile strength: almost 8 MPa	Around 52	1% (w/w)	N.A.	*In vitro* and *in vivo*	221
TPU/MWNT nanofibrous scaffolds	Rat mesenchymal stem cells	Elastic modulus: 10.01 MPa	Tensile strength: 17.21 MPa, tensile strain: 125%	N.A.	2.5 wt%	N.A.	*In vivo*	222
Poly(NIPAM-*co*-β-CD)/CNT/PPY hydrogel	N.A.	Storage modulus: 357 Pa, modulus: 93.0 ± 9.0	Tensile stress: 0.18 ± 0.02 MPa	N.A.	100 mg	N.A.	*In vitro*	223
Poly(3-hydroxybutyrate)-chitosan-MWNT/silk scaffold	N.A.	N.A.	Tensile strength of aligned: 48.13 ± 2.2 MPa Tensile strength (random): 46.68 ± 5.95 MPa	Above 80	1 wt%	N.A.	*In vitro*	224

Table 2 (*Contd.*)

Composite structure	Type of tissue	Modulus	Strength	Porosity, %	Optimum amount of CNTs	Cell viability, %	Model(s)	Ref.
MWCNTs and SWCNTs/PHBV composites	Bone	N.A.	Flexural strength: SWCNT: around 60 MPa/MWCNTs: around 58 MPa	N.A.	4 wt%	N.S (0.4)	*In vitro* and *in vivo*	225
MWCNTs/GEL-CS nanocomposites	Bone or cartilage	Tensile modulus: around 330 MPa	Tensile strength: 55 MPa	N.A.	1.0 g	N.A.	*In vitro*	226
HA/HDPE/MWCNT	Bone	N.A.	Flexural strength: around 150 MPa	N.A.	1%	N.A.	*In vitro*	227
CS/gel/nHAp/0.6% MWCNTs scaffolds	Bone	Elastic modulus: around 6.5 MPa	N.A.	Around 90	0.6%	OD: around 1.5	*In vitro*	228
CS–HAp–MWCNT	Bone	Young's modulus *ca.*: 4.88 GPa	Tensile strength *ca.* 76.21 MPa	N.A.	0.5 wt%	Around 90	*In vitro*	229
PVA/BCP scaffold	Bone	Elasticity modulus: 681 kPa	Compressive strength 81 ± 6 kPa	80% ± 0.6%	0.25%	N.A.	*In vitro*	230
MWCNTs/nHA/PCL composite	Bone	Modulus: nearly 95%	Compressive strength: 32.4 ± 1.6 MPa, tensile strength: 30.0 ± 1.4 MPa	N.A.	1 wt%	N.A.	*In vitro*	231
G/Ch scaffolds with two ratios (2 : 1 and 3 : 1)	Bone	Compressive modulus: 18.7 MPa, elastic modulus: 18 723 kPa	Compressive strength: 411 kPa	∼91	0.05 wt%	N.A.	*In vitro*	232
BMP-6/CCM scaffold	Calvarial bone	Compressive modulus: 0.84 ± 0.08 MPa	Compressive strength: 10.06 ± 0.07 MPa	80.66 ± 1.99	1.5%	N.A.	*In vivo*	233

weight-polyethylene (UHMWPE), MWCNTs, and nanosized hydroxyapatite (nHA) was developed for biomedical applications in tissue engineering of bone/blood cells. According to the mechanical tests, the addition of MWCNT had effects such as increasing the yield strength, work of fracture, and porosity up to ~16.9 ± 0.6 MPa, 4.7 ± 0.2 J, and 8.6%, respectively. These properties strengthened the composite to enable it to resist the physiological environment and support the growth of stem cells, osteoblasts for the articulation of the femoral head, and the expression of rouleaux formation of RBCs.[190]

Conductive scaffolds are a suitable option for cardiovascular tissue engineering due to their similarity to the ECM of native tissue. For example, Mombini *et al.* fabricated chitosan–polyvinyl alcohol (PVA)–CNT nanofiber scaffolds with different percentages of CNTs with an optimal diameter of 255 ± 3.5 nm for cardiomyocyte differentiation. The presence of CNTs, in addition to increasing the conductivity, caused a significant increase in porosity (70% to 80% on average) and an increase in elastic modulus and tensile strength to 130 ± 3.605 and 4.9 ± 1.961, respectively. This led to the creation of a 3D platform for the proliferation and growth of cells and increased the adhesion of MSCs to the scaffold.[191] The sufficient strength of biomaterials is essential in the field of tissue engineering because high strength damages soft tissues and tissue regeneration, while low strength causes rapid collapse, and thus the mechanical properties of the scaffold are vital. Finally, it can be said that CNTs, as biologically active molecules, have unique potential for different types of tissue engineering because by introducing their inherent mechanical properties in the scaffold, they can promote ECM expression and improve the substrate to stimulate cell growth and repair.[192–194]

Table 2 presents some reports concerning the mechanical features of CNT-based composites used in tissue engineering.

3.3. Fibrous carbon nanostructures

Fibrous carbon nanostructures are considered one of the most important structures in enhancing physical attributes including mechanical properties due to their exceptional morphology.[234] The most common way to produce fibrous structures is electrospinning.[235] CFs are also known for their good electrical and thermal conductivity.[236] Together with CFs, other types of fibrous carbon nanostructures, such as CNTs, multi-wall CNTs (MWCNT), and GO, are also investigated in this section.[237,238]

CFs exhibit excellent mechanical, thermal, and electrical properties, and therefore have great potential for a variety of biomedical applications, including tissue engineering. Carbon nanofibers (CNFs), as a category of CFs, have a higher length-to-diameter ratio than CNTs. They also show significant mechanical properties and can act as reinforcements to increase the tensile and compressive strain limits of materials.[236] In addition, nanofibrous structures can serve as an efficient framework for cell adhesion, proliferation, and differentiation, which differentiates them from other forms of nanomaterials.[239]

Improved mechanical property is an important factor in many materials used in biological applications, such as dental and orthopedic implants. In this regard, Han *et al.* combined the mechanical properties of polyether-ether-ketone (PEEK) with CFs using fused deposition modeling (FDM) printing technology and prepared CF-reinforced PEEK (CFR-PEEK) composites. The mechanical tensile, bending, and compressive strength improved from 95.21 MPa, 140.83 MPa, and 138.63 MPa to 101.41 MPa, 159.25 MPa, and 137.11 MPa respectively, which indicates that compared to pure PEEK, CFR-PEEK has much higher mechanical strength and can be used as a great candidate for dental and orthopedic implants in bone grafting and tissue engineering applications. Moreover, biological tests exhibited good biocompatibility for biological applications.[240]

Generally, PEEK is considered a suitable polymer for soft and hard tissue engineering due to its physical and chemical properties such as stability and radiolucency. However, it has a lower elastic modulus in the range of 3.7–4 GPa compared to that of human cortical bone of 7–30 GPa.[241] In this case, CFs can be used to increase the stiffness of PEEK and enhance its utilization. For instance, Uddin and coworkers designed highly porous PEEK foams with CFs, carbon nanotubes, and hydroxyapatite (HA) particles through cast melting and salt porogen leaching techniques and used them as bone scaffold materials. The results showed that with the incorporation of these nanoparticles in the composites, the modulus and yield strength significantly increased, making them good candidates for biological applications, including bone regeneration and scaffolding.[242] For instance, Naskar *et al.* fabricated bio-nanocomposites based on silk protein fibroin and reinforced them with CFs. These composites where further used for bone-tissue engineering applications. The addition of CF increased the compressive modulus by about 4.3-times compared to the control fibroin sponges. Besides having good mechanical properties, these composites were shown to be biocompatible and non-hemolytic.[243] Using the electrospinning technique, other types of carbon nano-structures can be incorporated in fibrous systems. Mahmoodi and coworkers designed a PCL/keratin (Kr)/CNT scaffold using electrospinning to study the effect of CNTs-COOH on the fibrous scaffold in hard tissue engineering applications. The incorporation of nano carbon led to a decrease in the fiber diameter from 123 to 55 nm and an increase in porosity and mechanical tensile strength from 3 MPa for PCL/Kr to 8 MPa for PCL/Kr/CNT. The CNT-containing scaffolds showed more cell adhesion and growth due to their higher special surface area and hydrophilicity compared to the untreated PCL/Kr scaffolds.[25]

Generally, PCL is considered a frequently used polymer in biological applications.[244] Tohidlou and coworkers embedded an amine-functionalized single-walled carbon nano-tube (aSWCNT) in PCL scaffolds for bone tissue engineering applications. By adding 0.2% of aSWCNT to PCL, the tensile strength increased from 1.6 MPa for pure PCL to 9.3 MPa for aSWCNT/PCL, which is very considerable. Also, the incorporation of aSWCNT led to an increase in cell proliferation, adhesion, and stem cell differentiation, together with the bioactivity and biodegradation rate of the biomaterial.[33] In a different study, Abdal-hay and colleagues used air jet spinning to fabricate PCL nanofibers incorporated with MWCNTs. The tensile strength

increased from 0.382 ± 0.1 for pure PCL to 0.483 ± 0.12 for PCL/1% MWCNT. Also, the tensile elastic modulus increased from 17 ± 3.5 for PCL alone to 110 ± 41.8 for PCL/0.5% MWCNT and 650 ± 74.5 for PCL/1% MWCNT nanofibers.[245]

Mechanical strength is an important factor in cardiac tissue engineering as well as hard tissue engineering. The implanted scaffolds used in this specific application must be able to recapitulate the environment of the heart.[246] To achieve an effective scaffold for cardiac tissue engineering, Abedi and coworkers fabricated electro-conductive scaffolds based on chitosan (CS), PVA, and MNCNTs using electrospinning. Further, USSC stem cells were cultured on these scaffolds and were pushed into desired differentiation path using small molecules and electrical stimulation. The addition of 2% of MWCNT to this fibrous structure caused a decrease in the fiber dimeter by 115 nm and an improvement in tensile strength and their conductivity from 8×10^{-5} S m^{-1} to 9×10^{-3} S m^{-1}, which are considered crucial factors for this application (Fig. 6).[32]

In cardiac tissue engineering, the scaffold must mimic the native environment of the body with factors such as similar conductivity and mechanical behaviour.[247] Therefore, incorporating conductive materials in scaffold structures can be beneficial to their behaviour. Considering their conductivity and appropriate mechanical properties, CNTs have shown interesting potential for these applications. To overcome limitations with the incorporation of these particles, Jiang and coworkers electrospun PCL/gelatin into a CNT bath and fabricated textile-based scaffolds using the resulting yarns. The test results showed that the incorporation of CNTs influenced the thermal and mechanical properties of the scaffolds. The yarns where also biocompatible and could guide cell elongation and alignment. The textile fabric resulting from these yarns was tested as a vascular scaffold, showing mechanical properties similar to native vessels.[30]

Another carbon nano-structure that can be incorporated in a fibrous structure is GO. GO is known for its hydrophilicity and conductivity and once combined with the appropriate material, it shows potential for different types of tissue engineering. For instance, Öztatlı *et al.* designed a PLLA/GO scaffold using electrospinning and tested its potential for nerve regeneration applications. PLLA is biocompatible and easy to shape but it also is hydrophobic and lacks proper binding sites. Accordingly, the addition of GO improved the physical, chemical, and mechanical properties of the scaffold including tensile and water contact angle, making it appropriate for nerve tissue engineering. By adding 10% of GO to the composite, the tensile strength increased up to 12.93 MPa, which was significantly higher than that of the neat PLLA nanofibers with a tensile strength of 2.25 MPa.[248]

Cartilage tissue, as a connecting tissue, plays an important role in protecting joints and bones. However, its injury is very common and it does not possess high regeneration capability. Therefore, it is necessary to develop new technologies and methods for the treatment of this important tissue.[249] In this regard, Golshayan *et al.* used the electrospinning method to prepare poly(3-hydroxybutyrate)–chitosan/functionalized

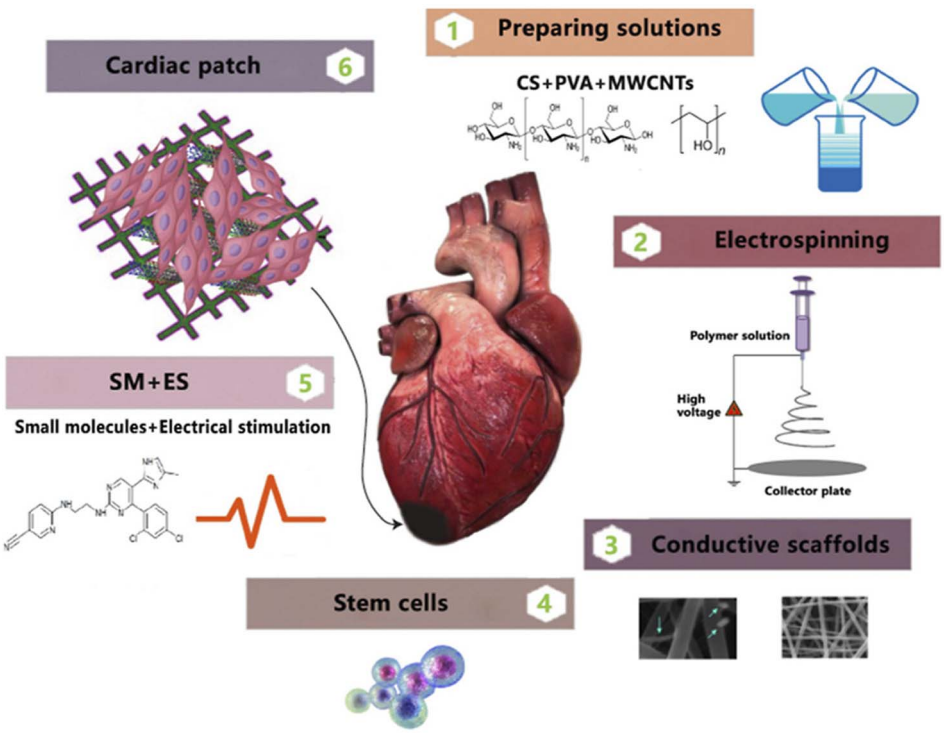

Fig. 6 (1–3) The preparation of electrospun scaffolds based on CS, PVA, and MWCNTs; (4) culturing USSC stem cells; (5) applying small molecules and electrical stimulation; and (6) the preparation of cardiac patches by combining the above-mentioned factors. Reprinted with permission from ref. 32 Elsevier, copyright 2021.

MWCNT (PHB–CS/f-MWCNT) with glucosamine sulfate (GAS) and tested its capabilities for cartilage tissue engineering. GAS is considered an important factor in cartilage tissue extracellular matrix and it improved the hydrophilicity of the fiber. Furthermore, the addition of CS to PHP decreased the Young's modulus from ~4.71 to ~4.20 MPa, while after the addition of nanotubes, this number increased to ~7.24 MPa. The combination of the scaffolds with GAS decreased the tensile modulus slightly but the composite still had sufficient strength for cartilage tissue engineering application.[250]

Generally, one of the most important factors in designing new composites for different types of tissue engineering is that the designed composite must show similar mechanical properties with the target native tissue. For example, Deng and coworkers designed a novel composite consisting of CF, HA, and polyamide46 (PA46) and tested its mechanical properties and biocompatibility for bone repair applications. The addition of CF increased the bending strength from ~116 to 159–223 MPa, tensile strength from ~95 to 127–199 MPa, and tensile modulus from ~4.6 to 7.7–10.8 GPa. The incorporation of CF also had positive effects on the biocompatibility of MG63 cells, indicating the potential of this composite for bone tissue engineering application.[251] Using the electrospinning technique, Zhang and coworkers prepared CS/PVA/astaxanthin (ASTA) nanofibers and evaluated their morphological and mechanical properties together with biocompatibility and cytotoxicity. The addition of GO led to a decrease in the diameter of the nanofibers and mechanical tensile strength from 2.57 MPa to 2.24 MPa, which was further elevated up to 3.39 by adding ASTA to the fibrous structure. Bacteriostatic and cytotoxicity tests also showed *Escherichia coli* growth inhibition and good cell compatibility.[252]

Interestingly, the size differentiation appears to be nondecisive in the biocompatibility rate of fibrous carbons. For instance, Grabinski *et al.* prepared CFs and carbon nanofibers with different sizes and diameters (10 μm to 100 nm), which showed no significant cytotoxicity in a cell viability test.[253]

In conclusion, CFs can be beneficial in increasing the mechanical properties of composites used in different types of tissue engineering.[254] They can be added to different materials to overcome their mechanical limitations.[255] Moreover, by incorporating different types of carbon nanostructures in fibrous systems, their mechanical properties can be altered as desired for specific tissue engineering applications.[256,257]

3.4. Nanodiamonds

NDs, which are carbon-based nanomaterials with a tetrahedral structure and sp^3 hybridization, are gaining traction in the biomedical field due to their high biocompatibility, simple surface functionalization, bright fluorescence, antimicrobial activity, chemical inertness, and superior mechanical properties including hardness, Young's modulus, high-pressure resistance, and great fracture toughness.[258–260] ND composites include polymer components and types of NDs. The use of NDs increased the mechanical strength, thermal stability, elastic modulus, and tensile strength of biodegradable polymers.[261] The fabrication of an appropriate biocompatible and biodegradable scaffold with mechanical strength similar to human bone is the primary challenge in bone tissue engineering. Recently, among the common bone implant materials (titanium), the ability of coatings containing diamond to increase the bone integrity, reinforce the mechanical properties of implants, ease the surface chemistry, and provide antimicrobial properties has been studied in the field of orthopedic implants.[258]

Furthermore, recent studies have revealed the effect of various designing methods of diamond lattice on penetrability, successful cell culture, proper elastic modulus, *etc.*[262] Following this investigation, Timercan *et al.* prepared lattice systems of gyroid and diamond that were mechanically flexible and penetrable to liquids, thus encouraging osseointegration and decreasing complexity risks, for instance, a lack of fixation, device migration, and subsidence in current intervertebral fusion devices. These structures were manufactured using Ti–6Al–4V and laser powder bed fusion. The Sy/*E* of the lattice structures ($25–33 \times 10^{-3}$) was considerably better than that of the bulk metals ($\sim 10 \times 10^{-3}$ for Ti–6Al–4V). Compared to Ti–6Al–4V, the modulus of elasticity and mechanical resistance were 1.9–4.8 GPa and 52–160 MPa (*i.e.*, a 24–60-fold decline in Young's modulus, *E*, and 7–21-fold decline in yield stress), respectively.[263]

Besides, the surface of ND has an influential function in the design of utility and biocompatibility in the biological field. A combination of covalently functionalized UNCD surface, biocompatibility, and superior mechanical properties led to the use of UNCD as a hermetic coating for implantable artificial retina devices and as a guide to improve neural stem cell transplantation and neural tissue regeneration.[264] In an important study, Liskova *et al.* revealed that O-terminated NCD films with high mechanical hardness and chemical resistance increased osteogenic cell differentiation and cell adhesion and growth.[265] Element doping is the primary method for solving insufficient adhesion and bioinertness in carbon films, particularly DLC and a-C films. The design of a multifunctional Cu/a-C:H thin coating deposited on the Ti–6Al–4V alloy (TC4) *via* magnetron sputtering in the presence of Ar and CH_4 for applications in bone implants was reported by Milan and coworkers. The results of the test revealed that with an increase in the copper concentration in a-C:H coatings, the ratio of sp^2/sp^3 also increased, and the interior stress intensity of the Cu/a-C:H biofilms decreased. Furthermore, with an increase in Cu concentration (from 30 wt% to 37 wt%), the Young's modulus decreased significantly from 88 GPa to 25 GPa; however, the hardness increased considerably from 7.8 GPa to 10 GPa. In Cu/a-C:H films with an increasing Cu content, arteries develop on the titanium alloy surface, which increases the likelihood of implants succeeding.[266]

Investigations on the shear modulus variations as a function of the volume of ND in hybrid substances indicated that the shear modulus of new nanocomposites comprised of pHEMA and NDs at concentrations 2% to 5% volume as a biomimetic biomaterial was comparable to that of the cortical bone (10–20 GPa). In the case of nano silica hybrids, similar results were

Table 3 Mechanical properties of ND-based composites in tissue engineering

Composite Structure	Type of tissue	Modulus	Strength	Porosity, %	Optimum amount of NDs	Cell viability, %	Model(s)	Ref.
ND-OAD/PLLA	Bone marrow	Young's modulus: 7.9 GPa	N.A.	N.A.	10 wt%	N.A.	*In vitro*	260
n-DP-PLA/poly (LLA-*co*-CL)	Bone	112.1 MPa	N.A.	92.2%	10 wt%	N.A.	*In vitro*	261
Nb-C film	Bone mouse calvaria	Young's modulus: 191.7 GPa	N.A.	N.A.	52.1 wt%	N.A.	*In vitro*	270
PVDF/BG scaffold	Bone	N.A.	Tensile strength: 59.61 MPa	N.A.	1 wt%	N.A.	*In vitro*	271

obtained in higher concentrations of about 15% to 30% volume. Therefore, it is expected that hybrid nanocomposites possessing higher mechanical strength, biomimetic, osteoconductivity, and osteoinductivity properties, while overcoming the main weakness of hydrogels (*i.e.*, poor mechanical characteristics) are suitable candidates for applications in cartilage cell tissue engineering.[267,268]

Nanocellulose/nanocarbon composites are another type of new hybrid materials proposed for biomedical applications, particularly for wound dressing. A CS/BC composite was prepared using chitosan-based biopolymers containing 33 wt% bacterial cellulose and 1 to 3 wt% MND. The mechanical properties of mats significantly increased by adding 1 wt% MND particles. Also, the ductility loss, elastic modulus (458 MPa), and yield strength (25.3 MPa) of the fibers increased and were close to that of natural skin. The results of the MTT assay demonstrated on L929 fibroblasts cultured on electrospun composite nanofibrous mats that the cell viability after a one-day incubation was higher than 90% compared with the control.[259,269]

A summary of the reports on ND-based composites and their mechanical properties in tissue engineering is shown in Table 3.

3.5. Other carbon-based nanocomposites

Other nanocarbon materials that can reinforce and modify the mechanical properties of nanocomposites include fullerenes, carbon black, active carbon (also called activated charcoal), CDs, and CQDs. Recently, a considerable number of studies focused on the use of nanocomposites based on these nanocarbons, which is ascribed to their extraordinary structural, electronic properties and high mechanical stability. Due to their features such as unique porosity with a large surface area/volume ratio, higher tensile strength and electrical conductivity, excellent solubility in water, high cell penetration ability, and acceptable biocompatibility, nanocarbon materials have been widely used in nanocomposites operated for a variety of biomedical purposes including drug delivery, wound dressing, bioimaging, and tissue engineering. Among these materials, one of the most attractive is fullerenes. Fullerenes are allotropic forms of carbon and exist in various forms, depending on the number of carbon atoms present in the molecule such as C_{60}, C_{70}, C_{80}, and multi-layer fullerenes, which are described as carbon nano-onions (CNOs). The biological application of fullerene nanomaterials expands new scientific frontiers in tissue engineering. The biodegradable CS/PVA/ox-CNO scaffolds with potent biomedical applications were developed by Tovar *et al.* In this study, they used five different formulations of CS/PVA/ox-CNOs and evaluated their properties to achieve a targeted scaffold for tissue engineering. Studying the degradation of samples in an SBF showed that the samples without ox-CNOs lost 75% and 85% of their weight after 15 days, while the *in vivo* tests showed that after 90 days of subcutaneous implantation of films containing ox-CNOs in the tissue of Wistar rats, only partial degradation occurred without any immune responses and allergic reactions. All the results illustrated the biocompatibility of CS/PVA/ox-CNOs and strongly assured that the presence of ox-CNOs not only stabilized the films through chemical interactions with the CS/PVA chains, but also delayed the degradation. Alternatively, mechanical tests were performed for five different as-fabricated formulas, which showed an ascending trend in Young's modulus and tensile strength of the CS/PVA/ox-CNOs samples compared to CS/PVA composites. The hydrogen bond between the chitosan amino groups and carboxyl groups on the ox-CNO surface increased the tensile strength of the nanocomposite. Consequently, ox-CNO acts as an absorber of part of the mechanical stress imposed on the nanocomposite and amends the tensile strength. Incorporating low amounts of ox-CNOs (0.25, 0.50, and 0.75 wt%) in the CS/PVA composite created disorder and resulted in the loss of crystallinity and decreased Young's modulus. Besides, increasing the content of ox-CNO, caused an adequate and uniform dispersion of ox-CNO, stress harmonious distribution, modification of crystallinity (confirmed by XRD analysis), and finally an increase in Young's modulus. Thus, based on the results, the CS/PVA/ox-CNOs nanocomposite can be considered a conducive scaffold for skin tissue engineering.[272] Following this investigation, Vedhanayagam and coworkers functionalized CBNs (including GO, rGR, fullerene C_{60}, and CNT) with TES-PAMAM-G_3, and then cross-linked collagen in them. These scaffolds were investigated as candidates for wound healing and tissue engineering in soft- and high-load bearing application. Compared to pure collagen, the CBN-TES-PAMAM-G_3 cross-linked collagen showed a higher Young's modulus (close to natural bone tissue) and tensile strength, biocompatibility, controlled swelling, and enhanced

degradability.[273] In addition to fullerenes, other carbon nanoparticles utilized in biomedical applications include CB and AC. CB is a type of paracrystalline carbon that has a large surface-to-volume ratio, although this ratio is lower than AC. Activated carbon is a graphite-like and processed form of carbon with high porosity.[259,274] Besides mechanical properties, conductive scaffolds based on CBNs have received significant attention due to the transmission of the electrical signal necessary to regulate cell behaviour in the engineering of tissues such as nerves, bone, and heart, which are electrically active. For example, Kai and coworkers developed a porous, hybrid memory-shape scaffold using PDMS and PCL blended with various amounts of CB. The results indicated that the addition of CB to the poly(PCL/PDMS urethane) nanofibers slowly increased the tensile strength (*i.e.*, from 4.22 MPa for neat polymer to 4.81 MPa for CB-based nanofiber), while considerably decreasing the elongation and Young's modulus. Furthermore, the good biocompatibility, low degradation rate, intact morphology, increased electrical conductivity with an increase in CB content in the fibers and biostability make this a promising scaffold for nerve tissue engineering.[275] In a recent study, the fabrication of the PAN/nCB/HA nanocomposite *via* electrospinning was presented by Haider *et al.* as a bioactive platform in bone tissue engineering. A substantial improvement in Young's modulus and tensile strength was observed in PAN/HA by incorporating 1 wt% nCB. This is because the polymer chains and CB nanoparticles interact strongly. Although there was a downward trend in Young's modulus and tensile strength with a change in the content of HA (from 5 wt% to 15 wt%), these values were still higher for PAN/nCB/HA than that without nCB. With the addition of nCB and HA to the PAN membrane, the swelling ratio increased, which can be related to the higher porosity of the scaffold, and also more hydroxyl groups on the surface. Overall, scaffolds based on nCB/HA can be successful in the regeneration of bone and other hard tissue.[276,277] The *in vitro* biological assay of porous PVA-AC nanocomposites in osteoblast MG 63 cells showed that the PVA-AC scaffold facilitated osteoblast differentiation, cell proliferation, and cell growth without the addition of any extra growth factor. The findings of this research revealed that the modification of the polymer matrix with AC reinforcing agent improves the mechanical properties without disrupting the scaffold porosity as well as biological properties. Interestingly, the prepared scaffold has advantages in terms of morphology and porosity, which are essential for handling cell migration and transport of nutrients to the cells by allowing osteoblast growth inside the scaffold without cytotoxic effects. According to the mechanical behaviour assay, the presence of 2.5 wt% AC in the polymer matrix resulted in more than a 207% enhancement in tensile strength and 349% in Young's modulus, which was related to the homogeneous dispersion of AC with an increase in its concentration (from 0.5 wt% to 2.5 wt%) and effective stress transfer in the polymer matrix. Consequently, the obtained innovative nanocomposite demonstrated the applicable role of AC in bone tissue engineering.[278] C-dots have emerged as a new class of fluorescent nano-sized carbon-based materials (<10 nm in size). These zero-dimensional carbon nanoparticles consist of carbon atoms with sp^2 and sp^3 hybridization in a quasi-spherical shape.[279,280] Recently, the applications of C-dots as highly potential bone tissue engineering scaffolds and in diagnosis and therapies of bone-related diseases have been widely examined.[281] Accordingly, the fabrication of a CD-decorated HAp/PU nanocomposite using waste and bio-based resources was designed as a tremendous potential bone regenerating scaffold by Gogoi *et al.* The CD-decorated HAp resulted in increased cell proliferation and deep cell adhesion and had no negative effect on osteoblast cells according to the cytotoxicity evaluations. The uniform dispersion of CD–HAp and strong interactions between the surface substitutions of the CDs and PVA chains through hydrogen bonding without any agglomeration in the matrix led to an increase in tensile strength, scratch hardness, and toughness, as calculated using the stress–strain curve of the CD–HAp/PU nanocomposites. Also, the layered structure of CD added to the polymer matrix improved the elongation at break of CD–HAp/PUs, followed by good flexibility, which is one of the requirements of bone implant materials.[282] Numerous researchers have incorporated CBNs in hydrogels to enhance their biological, mechanical properties, and electrical conductivity, making them targeted nanoplatforms in biomedical applications.[283] For example, the mechanical properties of as-prepared CD/HA/PVA double-network (DN) hydrogels were investigated based on the changes in three factors, including CD to PVA mass ratio (at 0.0, 1.5, 3.0, 4.5 and 6.0 wt% from CDs), HA to PVA (at 0.0, 0.2, 0.4, 0.6 and 0.8 wt% from HA) and the number of freezing/thawing cycles (from 0 to 9 cycles). Generally, after achieving the optimal conditions based on the above-mentioned parameters, the $CDs_{3.0}/HA_{0.6}$/PVA DN_9 hydrogel exhibited excellent compression mechanical properties, *i.e.*, compression strength of 3.462 MPa (about 477% increase) at a strain of 80%, and a notable enhancement of 429% in Young's modulus (4.5 kPa), introducing it as an outstanding potential cartilage/bone replacement in the field of biomedical engineering.[284] Considering the presence of –OH groups in the structure of CDs, they highly influence the hydrophilicity and swelling ratio of the gel. Therefore, the CD/HA/PVA DN hydrogels with more freezing/thawing cycles exhibited a higher crosslinking density, and therefore decreased crosslinking ratio. In an interesting study, Ghanbari *et al.* developed chemically cross-linked OA/GEL/CNQD hydrogels based on OA, GEL, and CNQDs (with 0.06% CNQDs) as conducive scaffolds for injection in the regeneration of damaged cartilage tissue due to their cell viability (>97%), enhanced cell adhesion on MG 63 cells, and mechanical durability.[285] Another study by Rastegar and coworkers described a notable improvement in tensile strength (5 MPa), Young's modulus (11 MPa), and elongation at break (10 mm) of a multifunctional PGS/PCL/CQD scaffold with the optimized weight ratio (2 : 1 : 0.5) compared to PGS/PCL. Thus, the enhancement in mechanical and biological properties and electrical conductivity mainly created by the addition of CQDs make the PGS/PCL/CQD nanocomposite an immensely promising material for cardiac tissue engineering.[286]

4. Advantages and disadvantages of carbon-based nanocomposites regarding mechanical properties in tissue engineering applications

The proliferation and migration of cells are dependent on the physicochemical interplay between cells and the surrounding extracellular matrix.[287] Consequently, the mechanical properties of carbon-based nanomaterials used in tissue engineering play a vital role in affecting cellular behaviour. It was observed that cells cultured on substrates possessing greater stiffness exhibited a greater modulus, as well as a more elongated and well-structured actin cytoskeleton,[288] and therefore the carbon-based nanocomposites utilized in the engineering of this tissue must exhibit sufficient mechanical strength to facilitate cellular growth and proliferation. In addition to possessing good mechanical properties, the scaffold used in tissue engineering must also provide sufficient porosity for cell growth. In this case, besides excellent mechanical strength, carbon-based nanomaterials exhibit notable porosity, which can accommodate cells and facilitate cellular infiltration.[289] Furthermore, carbon-based nanoscale scaffolds possess a high surface-to-volume ratio, thereby revealing a heightened probability of molecular interactions with cells.[290] Furthermore, the electrical property of carbon-based nanomaterials is an added advantage in tissue engineering, especially neural and cardiac regeneration. Electrical stimulation has the potential to activate numerous intracellular signaling pathways, thereby interfacing with the intracellular microenvironment, and subsequently affecting cellular processes such as migration, proliferation, and differentiation.[72] However, the presence of impurities, non-uniform morphology and structure, hydrophobicity, and insolubility of carbon-based nanomaterials represent impediments that pose significant challenges for tissue engineering and biomedical applications.[291]

In the field of biomedicine, the importance of water solubility and dispersibility cannot be overstated. Henceforth, it becomes indispensable to augment the hydrophilicity of carbon-based nanomaterials *via* diverse functionalization techniques, including the induction of covalent and non-covalent interactions.[292,293] Another disadvantage of carbon-based nanomaterials is the production of reactive oxygen species and oxidative stress, which increases their toxicity to living systems. There are various methods to decrease the toxicity of nanomaterials, and one of them is surface functionalization. This technique involves altering the surface of nanomaterials to minimize their interaction with biological systems.[294] Another method is encapsulation, which involves coating nanomaterials with a biocompatible substance to prevent them from interacting with biological systems. Additionally, managing the size and shape of nanomaterials can also minimize their toxicity.[295] Thus, considering the advantages and disadvantages of using carbon-based nanomaterials in tissue engineering, it can be concluded that carbon nanomaterials can be utilized as novel compounds in biomedical applications.

5. Conclusions

Carbon-based nanocomposites appear well-suited as biomaterials and may become useful tools in tissue engineering to combine with the host body. They can be utilized in applications such as cellular imaging, biological and chemical sensing, bioactive agent delivery, and matrix engineering. However, although the novel uses of carbon-based nanocomposites for biomedical applications are being expanded, there are concerns about their cytotoxicity, which can be mitigated by chemical functionalization. Engineered scaffolds made of carbon-based nanocomposites have effectively overcome many limitations of existing treatments owing to their useful attributes including biocompatibility, biodegradability, porosity, NIR optical features, and mechanical and electrical properties. Mechanical properties including elasticity modulus, tensile strength, elongation, hardness, density, creep, toughness, brittleness, durability, stiffness, creep rupture, corrosion and wear, low CTE, and fatigue limit, are considered one of the key issues in tissue engineering. Because engineered scaffolds made of carbon-based nanocomposites should accommodate long-term tissue regeneration and ensure the stability of local physiological structures *via* controlled biodegradability and the maintenance of appropriate mechanical performance during degradation, surgery is no longer required to remove them. The porosity of these carbon-based nanocomposites also creates a suitable microenvironment for cell adhesion and proliferation, which is vital for tissue regeneration.

Besides, these characteristics have shown a mutually restrictive relationship in *in vivo* and *in vitro* research. For instance, excessive porosity in carbon-based scaffolds may reduce mechanical strength. Conversely, too fast or too slow degradation may affect the repair. Therefore, the use of the appropriate dosage of carbon nanomaterials in composites and choosing the optimal production technique can lead to the preparation of scaffolds containing carbon nanomaterials that are more favorable for application in tissue engineering. Overall, carbon-based nanocomposites can be used as an important and unique component to impart the best mechanical properties to biomaterial to guide cell growth in combination with other biomaterials to potentially achieve tissue engineering goals.

Author contributions

R. Eivazzadeh-Keihan: conceptualization; visualization; validation; writing – original draft; writing – review & editing; project administration; supervision. Zahra Sadat: conceptualization; visualization; validation; writing – original draft; writing – review & editing. Farnaz Lalebeigi: formal analysis; data curation; conceptualization; visualization; validation; writing – original draft; writing – review & editing. Nooshin Naderi: formal analysis; data curation; visualization; validation; writing – original draft; writing – review & editing. Leila Panahi: conceptualization; visualization; validation; writing – original draft; writing – review & editing. Fatemeh Ganjali: visualization; validation; writing – original draft; writing – review & editing.

Sakineh Mahdian: formal analysis; data curation; validation; writing – original draft; writing – review & editing. Z. Saadatidizaji: data curation; validation; writing – original draft; writing – review & editing. M. Mahdavi: visualization; writing – original draft; and writing – review & editing. Elham Chidar: visualization; writing – original draft; and writing – review & editing. Erfan Soleimani: visualization; writing – original draft; and writing – review & editing. Azadeh Ghaee: formal analysis; validation; writing – original draft; writing – review & editing. A. Maleki: conceptualization; writing – original draft; validation; and writing – review & editing; project administration; supervision. Iman Zare: formal analysis; writing – review & editing; validation; project administration; supervision.

Conflicts of interest

The authors have reported no potential conflicts of interest.

Acknowledgements

The authors express their gratitude for the partial support received from the Research Council of the Iran University of Science and Technology.

Notes and references

1 W. Wang, Y. Shi, G. Lin, B. Tang, X. Li, J. Zhang, X. Ding and G. Zhou, *Macromol. Biosci.*, 2023, 2200539.
2 M. Kutz, *Mechanical Engineers' Handbook, Volume 4: Energy and Power*, John Wiley & Sons, 2015.
3 L. A. Carlsson, D. F. Adams and R. B. Pipes, *Experimental Characterization of Advanced Composite Materials*, CRC Press, 2014.
4 R. Eivazzadeh-Keihan, F. Radinekiyan, S. Asgharnasl, A. Maleki and H. Bahreinizad, *J. Mater. Res. Technol.*, 2020, **9**, 12244–12259.
5 H. Zhao, M. Liu, Y. Zhang, J. Yin and R. Pei, *Nanoscale*, 2020, **12**, 14976–14995.
6 R. Eivazzadeh-Keihan, F. Radinekiyan, H. Madanchi, H. A. M. Aliabadi and A. Maleki, *Carbohydr. Polym.*, 2020, **248**, 116802.
7 G. Wang, L. Liu and Z. Zhang, *Composites, Part A*, 2021, **141**, 106212.
8 Á. Serrano-Aroca, K. Takayama, A. Tuñón-Molina, M. Seyran, S. S. Hassan, P. Pal Choudhury, V. N. Uversky, K. Lundstrom, P. Adadi and G. Palù, *ACS Nano*, 2021, **15**, 8069–8086.
9 R. Eivazzadeh-Keihan, A. Maleki, M. De La Guardia, M. S. Bani, K. K. Chenab, P. Pashazadeh-Panahi, B. Baradaran, A. Mokhtarzadeh and M. R. Hamblin, *J. Adv. Res.*, 2019, **18**, 185–201.
10 N. Naderi, F. Lalebeigi, Z. Sadat, R. Eivazzadeh-Keihan, A. Maleki and M. Mahdavi, *Colloids Surf., B*, 2023, 113430.
11 A. Gholami, S. A. Hashemi, K. Yousefi, S. M. Mousavi, W.-H. Chiang, S. Ramakrishna, S. Mazraedoost, A. Alizadeh, N. Omidifar and G. Behbudi, *J. Nanomater.*, 2020, **2020**, 1–24.
12 N. Saini, P. Pandey, M. Shirolkar, A. Kulkarni, S.-H. Moh and A. A. Kulkarni, *Handbook of Porous Carbon Materials*, 2023, pp. 1151–1172.
13 P. Singh, K. R. Singh, A. K. Yadav, J. Singh, P. R. Solanki and R. P. Singh, in *Nanotechnological Aspects for Next-Generation Wound Management*, Elsevier, 2024, pp. 193–218.
14 Z. Sadat, F. Farrokhi-Hajiabad, F. Lalebeigi, N. Naderi, M. G. Gorab, R. A. Cohan, R. Eivazzadeh-Keihan and A. Maleki, *Biomed. Sci.*, 2022, **10**, 6911–6938.
15 Z. Peng, T. Zhao, Y. Zhou, S. Li, J. Li and R. M. Leblanc, *Adv. Healthcare Mater.*, 2020, **9**, 1901495.
16 M. Adel, P. Keyhanvar, I. Zare, Z. Tavangari, A. Akbarzadeh and M. Zahmatkeshan, *J. Drug Delivery Sci. Technol.*, 2023, **90**, 105130.
17 A. Haroun, Z. Gospodinova and N. Krasteva, *Nano Biomed. Eng*, 2021, **13**, 380–393.
18 L. S. Ulloa, F. Perissinotto, I. Rago, A. Goldoni, R. Santoro, M. Pesce, L. Casalis and D. Scaini, *Nanomater*, 2021, **11**, 2724.
19 K. Kaur, S. Sa'Paiva, D. Caffrey, B. L. Cavanagh and C. M. Murphy, *Mater. Sci. Eng., C*, 2021, **128**, 112340.
20 F. Chowdhury, M. Hosur and S. Jeelani, *Mater. Sci. Eng., A*, 2006, **421**, 298–306.
21 J. Zhu, W. Huang, L. Fu, B. Zhu, X. Li, X. Wang, Y. Wang and W. Chen, *ACS Appl. Nano Mater.*, 2021, **4**, 12453–12460.
22 R. Wazalwar, M. Sahu and A. M. Raichur, *Nanoscale Adv.*, 2021, **3**, 2741–2776.
23 D. L. Butler, S. A. Goldstein and F. Guilak, *J. Biomech. Eng.*, 2000, **122**, 570–575.
24 R. Eivazzadeh-Keihan, K. K. Chenab, R. Taheri-Ledari, J. Mosafer, S. M. Hashemi, A. Mokhtarzadeh, A. Maleki and M. R. Hamblin, *Mater. Sci. Eng., C*, 2020, **107**, 110267.
25 M. Mahmoodi, V. Haghighi, M. Mirhaj, M. Tavafoghi, F. Shams and A. Darabi, *Mater. Today Commun.*, 2021, **27**, 102401.
26 S. Zheng, Y. Tian, J. Ouyang, Y. Shen, X. Wang and J. Luan, *Front. Chem.*, 2022, **10**, 990362.
27 A. A. Al-Allaq, J. S. Kashan, M. T. El-Wakad and A. M. Soliman, *Mater. Technol.*, 2021, **55**, 673–680.
28 J. Wang, C. Huang, Y. Wang, Y. Chen, Z. Ding, C. Yang and L. Chen, *Colloids Surf., A*, 2020, **606**, 125520.
29 F. Velasco-Mallorquí, J. M. Fernández-Costa, L. Neves and J. Ramón-Azcón, *Nanoscale Adv.*, 2020, **2**, 2885–2896.
30 C. Jiang, K. Wang, Y. Liu, C. Zhang and B. Wang, *ACS Biomater. Sci. Eng.*, 2021, **7**, 2627–2637.
31 E. Díaz, J. Martín and J. León, *Compos. Interfaces*, 2021, **28**, 511–525.
32 A. Abedi, B. Bakhshandeh, A. Babaie, J. Mohammadnejad, S. Vahdat, R. Mombeiny, S. R. Moosavi, J. Amini and L. Tayebi, *Mater. Chem. Phys.*, 2021, **258**, 123842.
33 H. Tohidlou, S. S. Shafiei, S. Abbasi, M. Asadi-Eydivand and M. Fathi-Roudsari, *Fibers Polym.*, 2019, **20**, 1869–1882.
34 N. Saito, H. Haniu, K. Aoki, N. Nishimura and T. Uemura, *Adv. Sci.*, 2022, **9**, 2201214.
35 S. Loeve, in *Between Nature and Society: Biographies of Materials*, World Scientific, 2022, pp. 129–142.

36 R. S. Wils, N. R. Jacobsen, U. Vogel, M. Roursgaard and P. Møller, *Toxicol. Sci.*, 2021, **183**, 184–194.
37 S. Shamsi, A. A. Alagan, S. N. E. Sarchio and F. Md Yasin, *Int. J. Nanomed.*, 2020, 8311–8329.
38 M. d'Amora, M. Rodio, J. Bartelmess, G. Sancataldo, R. Brescia, F. Cella Zanacchi, A. Diaspro and S. Giordani, *Sci. Rep.*, 2016, **6**, 33923.
39 S. Bettini and G. Giancane, *Nanomaterials*, 2022, **12**, 2738.
40 N. Dhiman, S. Ghosh, Y. K. Mishra and K. M. Tripathi, *Mater. Adv.*, 2022, **3**, 3101–3122.
41 N. Panwar, A. M. Soehartono, K. K. Chan, S. Zeng, G. Xu, J. Qu, P. Coquet, K.-T. Yong and X. Chen, *Chem. Rev.*, 2019, **119**, 9559–9656.
42 M. Verdanova, B. Rezek, A. Broz, E. Ukraintsev, O. Babchenko, A. Artemenko, T. Izak, A. Kromka, M. Kalbac and M. Hubalek Kalbacova, *Small*, 2016, **12**, 2499–2509.
43 A. Isakovic, Z. Markovic, B. Todorovic-Markovic, N. Nikolic, S. Vranjes-Djuric, M. Mirkovic, M. Dramicanin, L. Harhaji, N. Raicevic and Z. Nikolic, *Toxicol. Sci.*, 2006, **91**, 173–183.
44 L. Zhang, J. Xia, Q. Zhao, L. Liu and Z. Zhang, *Small*, 2010, **6**, 537–544.
45 K.-H. Liao, Y.-S. Lin, C. W. Macosko and C. L. Haynes, *ACS Appl. Mater. Interfaces*, 2011, **3**, 2607–2615.
46 S. Vardharajula, S. Z. Ali, P. M. Tiwari, E. Eroğlu, K. Vig, V. A. Dennis and S. R. Singh, *Int. J. Nanomed.*, 2012, 5361–5374.
47 J. Wang, Z. Hu, J. Xu and Y. Zhao, *NPG Asia Mater.*, 2014, **6**, e84.
48 C. M. Sayes, F. Liang, J. L. Hudson, J. Mendez, W. Guo, J. M. Beach, V. C. Moore, C. D. Doyle, J. L. West and W. E. Billups, *Toxicol. Lett.*, 2006, **161**, 135–142.
49 M. Marzana, M. M. A. Khan, A. Ahmed, M. A. Jalil and M. M. Hossain, in *Nanomaterials for Biocatalysis*, Elsevier, 2022, pp. 689–714.
50 A. Rehman, S. Houshyar and X. Wang, *J. Biomed. Mater. Res., Part A*, 2020, **108**, 906–922.
51 Z. Xu, Y. Zhang, W. Zhou, L. Wang, G. Xu, M. Ma, F. Liu, Z. Wang, Y. Wang and T. Kong, *J. Nanobiotechnol.*, 2021, **19**, 1–11.
52 A. M. Schrand, L. Dai, J. J. Schlager, S. M. Hussain and E. Osawa, *Diamond Relat. Mater.*, 2007, **16**, 2118–2123.
53 Y. Kang, C. Wang, Y. Qiao, J. Gu, H. Zhang, T. Peijs, J. Kong, G. Zhang and X. Shi, *Biomacromolecules*, 2019, **20**, 1765–1776.
54 H. Mokhtari, M. Kharaziha, F. Karimzadeh and S. Tavakoli, *Carbohydr. Polym.*, 2019, **214**, 234–249.
55 B. Farshid, G. Lalwani, M. S. Mohammadi, J. S. Sankaran, S. Patel, S. Judex, J. Simonsen and B. Sitharaman, *J. Biomed. Mater. Res., Part A*, 2019, **107**, 1143–1153.
56 G. Choe, S. Oh, J. M. Seok, S. A. Park and J. Y. Lee, *Nanoscale*, 2019, **11**, 23275–23285.
57 R. Eivazzadeh-Keihan, F. Radinekiyan, A. Maleki, M. S. Bani, Z. Hajizadeh and S. Asgharnasl, *Int. J. Biol. Macromol.*, 2019, **140**, 407–414.
58 K. Krukiewicz, D. Putzer, N. Stuendl, B. Lohberger and F. Awaja, *Materials*, 2020, **13**, 2991.
59 M. Sabzevari, D. E. Cree and L. D. Wilson, *Mater. Chem. Phys.*, 2019, **234**, 81–89.
60 Z. Wright, A. Arnold, B. Holt, K. Eckhart and S. Sydlik, *Regener. Eng. Transl. Med.*, 2019, **5**, 190–209.
61 A. M. Díez-Pascual, in *Materials for Biomedical Engineering*, Elsevier, 2019, pp. 417–447.
62 C. S. Cabral, S. P. Miguel, D. de Melo-Diogo, R. O. Louro and I. J. Correia, *Carbon*, 2019, **146**, 513–523.
63 M. Li, Y. Miao, X. Zhai, Y. Yin, Y. Zhang, Z. Jian, X. Wang, L. Sun and Z. Liu, *Mater. Des.*, 2019, **181**, 107961.
64 A. Najafinezhad, H. Bakhsheshi-Rad, A. Saberi, A. Nourbakhsh, M. Daroonparvar, A. F. Ismail, S. Sharif, S. RamaKrishna, Y. Dai and F. Berto, *Biomed. Mater.*, 2022, **17**, 035011.
65 M. M. H. Rumon, S. D. Sarkar, M. M. Uddin, M. M. Alam, S. N. Karobi, A. Ayfar, M. S. Azam and C. K. Roy, *RSC Adv.*, 2022, **12**, 7453–7463.
66 K. N. Alagarsamy, S. Mathan, W. Yan, A. Rafieerad, S. Sekaran, H. Manego and S. Dhingra, *Bioact. Mater.*, 2021, **6**, 2261–2280.
67 P. Yılmaz, E. öztürk Er and S. Bakırdere, *J. Mater. Res. Technol.*, 2019, **8**, 5201–5216.
68 M. Vedhanayagam, B. U. Nair and K. J. Sreeram, *Materialia*, 2019, **7**, 100354.
69 M. K. Satapathy, Y. B. Manga, K. K. Ostrikov, W.-H. Chiang, A. Pandey, B. Nyambat, E.-Y. Chuang and C.-H. Chen, *ACS Appl. Mater. Interfaces*, 2019, **12**, 86–95.
70 X. Yao, Z. Yan, X. Wang, H. Jiang, Y. Qian and C. Fan, *Regener. Biomater.*, 2021, **8**, rbab032.
71 X. Qi, F. Jiang, M. Zhou, W. Zhang and X. Jiang, *Smart Mater. Med.*, 2021, **2**, 280–291.
72 M. Islam, A. D. Lantada, D. Mager and J. G. Korvink, *Adv. Healthcare Mater.*, 2022, **11**, 2101834.
73 S. Ghosh and K. Chatterjee, *Int. J. Nanomed.*, 2020, **15**, 5991.
74 S. D. Purohit, R. Bhaskar, H. Singh, I. Yadav, M. K. Gupta and N. C. Mishra, *Int. J. Biol. Macromol.*, 2019, **133**, 592–602.
75 R. Eivazzadeh-Keihan, E. Bahojb Noruzi, K. Khanmohammadi Chenab, A. Jafari, F. Radinekiyan, S. M. Hashemi, F. Ahmadpour, A. Behboudi, J. Mosafer and A. Mokhtarzadeh, *J. Tissue Eng. Regener. Med.*, 2020, **14**, 1687–1714.
76 H. Jodati, B. Yilmaz and Z. Evis, *Ceram. Int.*, 2021, **47**, 29535–29549.
77 R. Eivazzadeh-Keihan, F. Alimirzaloo, H. Aghamirza Moghim Aliabadi, E. Bahojb Noruzi, A. R. Akbarzadeh, A. Maleki, H. Madanchi and M. Mahdavi, *Sci. Rep.*, 2022, **12**, 6205.
78 M. Z. I. Nizami, S. Takashiba and Y. Nishina, *Appl. Mater. Today*, 2020, **19**, 100576.
79 L. Shang, Y. Qi, H. Lu, H. Pei, Y. Li, L. Qu, Z. Wu and W. Zhang, in *Theranostic Bionanomaterials*, Elsevier, 2019, pp. 165–185.
80 A. Maio, I. Pibiri, M. Morreale, F. P. L. Mantia and R. Scaffaro, *Nanomaterials*, 2021, **11**, 1717.
81 A. Sadeghianmaryan, Y. Karimi, S. Naghieh, H. Alizadeh Sardroud, M. Gorji and X. Chen, *Appl. Biochem. Biotechnol.*, 2020, **191**, 567–578.

82 J. Li, H. Zeng, Z. Zeng, Y. Zeng and T. Xie, *ACS Biomater. Sci. Eng.*, 2021, **7**, 5363–5396.
83 J. Sun, S. Shakya, M. Gong, G. Liu, S. Wu and Z. Xiang, *ChemistrySelect*, 2019, **4**, 5745–5754.
84 M. G. Tupone, G. Panella, M. d'Angelo, V. Castelli, G. Caioni, M. Catanesi, E. Benedetti and A. Cimini, *Int. J. Mol. Sci.*, 2021, **22**, 13047.
85 T. V. Patil, D. K. Patel, S. D. Dutta, K. Ganguly and K.-T. Lim, *Molecules*, 2021, **26**, 2797.
86 M. A. J. Maras, S. F. Rahman and G. W. Hardi, *AIP Conf. Proc.*, 2021, **2344**, 020014.
87 A. Montazeri, F. Saeedi, Y. Bahari and A. Ahmadi Daryakenari, *Polym. Polym. Compos.*, 2021, **29**, S926–S936.
88 C. Fu, Y. Jiang, X. Yang, Y. Wang, W. Ji and G. Jia, *Int. J. Nanomed.*, 2021, **16**, 6693.
89 C. Chen, Y. Xi and Y. Weng, *Materials*, 2022, **15**, 2164.
90 M. U. A. Khan, S. I. A. Razak, A. Hassan, S. Qureshi and G. M. Stojanović, *Front. Bioeng. Biotechnol.*, 2022, **10**, 865059.
91 S. J. Corr, M. Raoof, B. T. Cisneros, O. Kuznetsov, K. Massey, W. D. Kaluarachchi, M. A. Cheney, E. W. Billups, L. J. Wilson and S. A. Curley, *Nanoscale Res. Lett.*, 2013, **8**, 1–10.
92 M. Mazaheri, O. Akhavan and A. Simchi, *Appl. Surf. Sci.*, 2014, **301**, 456–462.
93 J. Shen, B. Yan, T. Li, Y. Long, N. Li and M. Ye, *Soft Matter*, 2012, **8**, 1831–1836.
94 A. Iakunkov, N. Boulanger, A. Nordenström and A. V. Talyzin, *Adv. Mater. Interfaces*, 2021, **8**, 2100552.
95 M. U. A. Khan, S. I. Abd Razak, H. Mehboob, M. R. Abdul Kadir, T. J. S. Anand, F. Inam, S. A. Shah, M. E. Abdel-Haliem and R. Amin, *ACS Omega*, 2021, **6**, 4335–4346.
96 M. M. Kadhim, D. O. Bokov, M. J. Ansari, W. Suksatan, M. A. Jawad, S. Chupradit, M. N. Fenjan and M. Kazemnejadi, *Bioprocess Biosyst. Eng.*, 2022, **45**, 981–997.
97 C. Shuai, B. Peng, P. Feng, L. Yu, R. Lai and A. Min, *J. Adv. Res.*, 2022, **35**, 13–24.
98 Y. Zhao, J. Chen, L. Zou, G. Xu and Y. Geng, *J. Chem. Eng.*, 2019, **378**, 122174.
99 S. Bahrami, N. Baheiraei and M. Shahrezaee, *Sci. Rep.*, 2021, **11**, 1–10.
100 M. Gong, J. Sun, G. Liu, L. Li, S. Wu and Z. Xiang, *Mater. Sci. Eng., C*, 2021, **119**, 111603.
101 M. A. Shamekhi, H. Mirzadeh, H. Mahdavi, A. Rabiee, D. Mohebbi-Kalhori and M. B. Eslaminejad, *Int. J. Biol. Macromol.*, 2019, **127**, 396–405.
102 V. Nazar, M. Kashi, M. Haghbin Nazarpak, E. Shahryari and M. Mehrjoo, *Int. J. Polym. Mater. Polym. Biomater.*, 2022, 1–12.
103 D. Trucco, L. Vannozzi, E. Teblum, M. Telkhozhayeva, G. D. Nessim, S. Affatato, H. Al-Haddad, G. Lisignoli and L. Ricotti, *Adv. Healthcare Mater.*, 2021, **10**, 2001434.
104 A. Mousavi, S. Mashayekhan, N. Baheiraei and A. Pourjavadi, *Int. J. Biol. Macromol.*, 2021, **180**, 692–708.
105 H. Nazari, A. Heirani-Tabasi, M. Hajiabbas, M. Khalili, M. Shahsavari Alavijeh, S. Hatamie, A. Mahdavi Gorabi, E. Esmaeili and S. H. Ahmadi Tafti, *Polym. Adv. Technol.*, 2020, **31**, 248–259.
106 M. Azizi, M. Navidbakhsh, S. Hosseinzadeh and M. Sajjadi, *J. Polym. Res.*, 2019, **26**, 1–9.
107 X. Zhao, Z. Zhang, J. Luo, Z. Wu, Z. Yang, S. Zhou, Y. Tu, Y. Huang, Y. Han and B. Guo, *Appl. Mater. Today*, 2022, **26**, 101365.
108 N. Abzan, M. Kharaziha and S. Labbaf, *Mater. Des.*, 2019, **167**, 107636.
109 R. Jaswal, S. Shrestha, B. K. Shrestha, D. Kumar, C. H. Park and C. S. Kim, *Mater. Sci. Eng., C*, 2020, **116**, 111213.
110 D. You, K. Li, W. Guo, G. Zhao and C. Fu, *Int. J. Nanomed.*, 2019, **14**, 7039.
111 A. Singh, S. L. Banerjee, V. Dhiman, S. K. Bhadada, P. Sarkar, M. Khamrai, K. Kumari and P. P. Kundu, *Polymer*, 2020, **195**, 122436.
112 A. Salleh, N. Mustafa, Y. H. Teow, M. N. Fatimah, F. A. Khairudin, I. Ahmad and M. B. Fauzi, *Biomedicines*, 2022, **10**, 816.
113 R. Al-Wafi, S. Mansour, M. AlHammad and M. Ahmed, *Int. J. Pharm.*, 2021, **601**, 120517.
114 M. U. Aslam Khan, A. Haider, S. I. Abd Razak, M. R. Abdul Kadir, S. Haider, S. A. Shah, A. Hasan, R. Khan, S. u. d. Khan and I. Shakir, *J. Tissue Eng. Regener. Med.*, 2021, **15**, 322–335.
115 P. H. M. Gohari, M. H. Nazarpak and M. Solati-Hashjin, *Mater. Today Commun.*, 2021, **27**, 102287.
116 M. Azizi, M. Kalantar, N. Nezafati and A. Zamanian, *J. Aust. Ceram. Soc.*, 2021, **57**, 947–960.
117 H. Rezaei, M. Shahrezaee, M. J. Monfared, S. F. Karkan and R. Ghafelehbashi, *J. Polym. Eng.*, 2021, **41**, 375–386.
118 A. Olad, H. B. K. Hagh, A. Mirmohseni and F. F. Azhar, *Ceram. Int.*, 2019, **45**, 15609–15619.
119 M. U. A. Khan, M. Rizwan, S. I. A. Razak, A. Hassan, T. Rasheed and M. Bilal, *J. Biomater. Sci., Polym. Ed.*, 2022, 1–20.
120 H. Belaid, S. Nagarajan, C. Teyssier, C. Barou, J. Barés, S. Balme, H. Garay, V. Huon, D. Cornu and V. Cavailles, *Mater. Sci. Eng., C*, 2020, **110**, 110595.
121 M. Narimani, A. Teimouri and Z. Shahbazarab, *Polym. Bull.*, 2019, **76**, 725–745.
122 Y. Du, M. Yu, W. Lu and J. Kong, *Composites, Part B*, 2021, **225**, 109270.
123 M. U. Aslam Khan, W. S. Al-Arjan, M. S. Binkadem, H. Mehboob, A. Haider, M. A. Raza, S. I. Abd Razak, A. Hasan and R. Amin, *Nanomaterials*, 2021, **11**, 1319.
124 M. Jafarkhani, Z. Salehi, Z. Bagheri, Z. Aayanifard, A. Rezvan, H. Doosthosseini and M. A. Shokrgozar, *Can. J. Chem. Eng.*, 2020, **98**, 62–68.
125 M. Ahmed, S. Mansour and R. Al-Wafi, *Biomed. Mater.*, 2021, **16**, 045030.
126 X. Li, J. Chen, Z. Xu, Q. Zou, L. Yang, M. Ma, L. Shu, Z. He and C. Ye, *J. Mater. Sci.: Mater. Med.*, 2021, **31**, 125.
127 A. Pourjavadi, Z. Mazaheri Tehrani, H. Salami, F. Seidi, A. Motamedi, A. Amanzadi, E. Zayerzadeh and M. Shabanian, *Polym. Eng. Sci.*, 2020, **60**, 889–899.

128 H. Lee, J. M. Yoo, N. K. Ponnusamy and S. Y. Nam, *Ceram. Int.*, 2022, **48**, 10155–10163.
129 A. Ali, A. Hasan and Y. S. Negi, *Int. J. Biol. Macromol.*, 2022, **197**, 1–11.
130 X. Lang, Z. Tang, Z. Wei, X. Wang, S. Long, G. Zhang, J. Yang and Q. Lin, *J. Innovative Opt. Health Sci.*, 2022, **15**, 2250007.
131 F. Liu, C. Liu, B. Zheng, J. He, J. Liu, C. Chen, I.-s. Lee, X. Wang and Y. Liu, *Polymers*, 2020, **12**, 69.
132 R. Mahdavi, G. Belgheisi, M. Haghbin-Nazarpak, M. Omidi, A. Khojasteh and M. Solati-Hashjin, *J. Mater. Sci.: Mater. Med.*, 2020, **31**, 1–14.
133 N. More, A. Srivastava and G. Kapusetti, *ACS Appl. Bio Mater.*, 2020, **3**, 6823–6835.
134 D. Kaya and N. Alemdar, *J. Appl. Polym. Sci.*, 2019, **136**, 46905.
135 M. Zou, J. Sun and Z. Xiang, *Adv. Healthcare Mater.*, 2021, **10**, 2001502.
136 M. R. Mahdavi, M. Kehtari, A. Mellati, R. N. Mansour, M. Mahdavi, M. Mahdavi and S. E. Enderami, *Cell Biochem. Funct.*, 2022, **40**, 203–212.
137 Z. Huang, Y. Wan, X. Zhu, P. Zhang, Z. Yang, F. Yao and H. Luo, *Mater. Sci. Eng., C*, 2021, **123**, 111967.
138 L. Wang, M. Fang, Y. Xia, J. Hou, X. Nan, B. Zhao and X. Wang, *RSC Adv.*, 2020, **10**, 10118–10128.
139 J. Zhu, Z. Qi, C. Zheng, P. Xue, C. Fu, S. Pan and X. Yang, *J. Nanomater.*, 2020, **2020**, 1–15.
140 P. Dorishetty, R. Balu, A. Gelmi, J. P. Mata, A. Quigley, N. K. Dutta and N. R. Choudhury, *Mater. Today Adv.*, 2022, **14**, 100233.
141 Y. Hou, W. Wang and P. Bártolo, *Int. J. Bioprint.*, 2020, **6**, 266.
142 C. Shen, J. Liu, Q. Lu, G. Wang, Z. Wang and L. Liu, *Int. J. Nanomed.*, 2022, **17**, 681.
143 Z. Jing, X. Xian, Q. Huang, Q. Chen, P. Hong, Y. Li and A. Shi, *New J. Chem.*, 2020, **44**, 10390–10403.
144 C. Qi, Y. Deng, L. Xu, C. Yang, Y. Zhu, G. Wang, Z. Wang and L. Wang, *Theranostics*, 2020, **10**, 741.
145 J. Xue, X. Wang, E. Wang, T. Li, J. Chang and C. Wu, *Acta Biomater.*, 2019, **100**, 270–279.
146 K. B. Narayanan, G. T. Park and S. S. Han, *Colloids Surf., B*, 2020, **191**, 110994.
147 X.-P. Li, K.-Y. Qu, B. Zhou, F. Zhang, Y.-Y. Wang, O. D. Abodunrin, Z. Zhu and N.-P. Huang, *Colloids Surf., B*, 2021, **205**, 111844.
148 Y. Wang, H. Yu, H. Liu and Y. Fan, *J. Bioact. Compat. Polym.*, 2020, **35**, 216–227.
149 C. Zhang, X. Wang, S. Fan, P. Lan, C. Cao and Y. Zhang, *Colloids Surf., B*, 2021, **197**, 111444.
150 S. Rethinam, A. W. Aruni, S. Vijayan, C. Munusamy and N. Gobi, *J. Drug Delivery Sci. Technol.*, 2019, **53**, 101163.
151 V. Kheiri Mollaqasem, A. Asefnejad, M. R. Nourani, V. Goodarzi and M. R. Kalaee, *J. Appl. Polym. Sci.*, 2021, **138**, 49797.
152 A. Xavier Mendes, S. Moraes Silva, C. D. O'Connell, S. Duchi, A. F. Quigley, R. M. Kapsa and S. E. Moulton, *ACS Biomater. Sci. Eng.*, 2021, **7**, 2279–2295.
153 W. Qin, C. Li, C. Liu, S. Wu, J. Liu, J. Ma, W. Chen, H. Zhao and X. Zhao, *J. Biomater. Appl.*, 2022, **36**, 1838–1851.
154 S. Mohammadi and A. Babaei, *Int. J. Biol. Macromol.*, 2022, **201**, 528–538.
155 J. H. Tsui, A. Leonard, N. D. Camp, J. T. Long, Z. Y. Nawas, R. Chavanachat, A. S. Smith, J. S. Choi, Z. Dong and E. H. Ahn, *Biomaterials*, 2021, **272**, 120764.
156 S. B. Ryu, K. M. Park and K. D. Park, *Biochem. Biophys. Res. Commun.*, 2022, **592**, 24–30.
157 M. H. Norahan, M. Pourmokhtari, M. R. Saeb, B. Bakhshi, M. S. Zomorrod and N. Baheiraei, *Mater. Sci. Eng., C*, 2019, **104**, 109921.
158 H. S. Budi, M. J. Ansari, S. A. Jasim, W. K. Abdelbasset, D. Bokov, Y. F. Mustafa, M. A. Najm and M. Kazemnejadi, *Inorg. Chem. Commun.*, 2022, **139**, 109336.
159 A. A. Aly and M. Ahmed, *Int. J. Pharm.*, 2021, **598**, 120325.
160 B. Huang, *Biomanuf. Rev.*, 2020, **5**, 3.
161 P. Yupapin, C. Mahesha, H. Fouladi, A. Hamidi and A. Farmani, *Silicon*, 2022, 1–7.
162 N. Anzar, R. Hasan, M. Tyagi, N. Yadav and J. Narang, *Sens. Int.*, 2020, **1**, 100003.
163 V. Kumar and H. Kumar, *Environ. Appl. Carbon Nanomater.-Based Devices*, 2021, 423–438.
164 T. V. Patil, D. K. Patel, S. D. Dutta, K. Ganguly, A. Randhawa and K.-T. Lim, *Appl. Sci.*, 2021, **11**, 9550.
165 J. M. Schnorr and T. M. Swager, *Chem. Mater.*, 2011, **23**, 646–657.
166 A. Kumar, K. Sharma and A. R. Dixit, *Carbon Lett.*, 2021, **31**, 149–165.
167 J. N. Coleman, U. Khan, W. J. Blau and Y. K. Gun'ko, *Carbon*, 2006, **44**, 1624–1652.
168 A. Raunika, S. A. Raj, K. Jayakrishna and M. Sultan, *IOP Conf. Ser.: Mater. Sci. Eng.*, 2017, **270**, 012027.
169 B. Portillo-Rodríguez, J. Sanchez-Vasquez, M. Reyes-Reyes and R. Lopez-Sandoval, *Diamond Relat. Mater.*, 2022, **121**, 108720.
170 R. Maheswaran and B. P. Shanmugavel, *J. Electron. Mater.*, 2022, 1–15.
171 S. Bosi, L. Ballerini and M. Prato, *Making and Exploiting Fullerenes, Graphene, and Carbon Nanotubes*, 2013, pp. 181–204.
172 R. Sorkin, A. Greenbaum, M. David-Pur, S. Anava, A. Ayali, E. Ben-Jacob and Y. Hanein, *Nanotechnology*, 2008, **20**, 015101.
173 X. Li, W. Yang, H. Xie, J. Wang, L. Zhang, Z. Wang and L. Wang, *ACS Appl. Mater. Interfaces*, 2020, **12**, 36860–36872.
174 J. Wang, L. Tian, N. Chen, S. Ramakrishna and X. Mo, *Mater. Sci. Eng., C*, 2018, **91**, 715–726.
175 T. Zhu, Y. Cui, M. Zhang, D. Zhao, G. Liu and J. Ding, *Bioact. Mater.*, 2020, **5**, 584–601.
176 C. Shuai, B. Peng, M. Liu, S. Peng and P. Feng, *Mater. Today Adv.*, 2021, **11**, 100158.
177 Z. Wang, L. Zhang, R. Zhang and M. Wang, *Mater. Lett.*, 2022, **315**, 131974.
178 S. Sang, R. Cheng, Y. Cao, Y. Yan, Z. Shen, Y. Zhao and Y. Han, *J. Zhejiang Univ., Sci., B*, 2022, **23**, 58–73.

179 M. E. David, R. M. Ion, R. M. Grigorescu, L. Iancu, A. M. Holban, F. Iordache, A. I. Nicoara, E. Alexandrescu, R. Somoghi and S. Teodorescu, *Nanomaterials*, 2022, **12**, 239.
180 X. Tong, J. Zheng, Y. Lu, Z. Zhang and H. Cheng, *Mater. Lett.*, 2007, **61**, 1704–1706.
181 M. Zhang, M. Yang, H. Nakajima, M. Yudasaka, S. Iijima and T. Okazaki, *ACS Appl. Nano Mater.*, 2019, **2**, 4293–4301.
182 E. Murugan, C. Akshata, V. Yogaraj, G. Sudhandiran and D. Babu, *Ceram. Int.*, 2022, **48**, 16000–16009.
183 M. L. Flores-Cedillo, R. Rosales-Ibáñez, M. Martin-del-Campo-Fierro, A. Reyes-Matute, J. V. Cauich-Rodríguez, L. A. Oros-Méndez, Á. L. Rodríguez-Morales and M. O. L. Flores-Sánchez, *Polym. Bull.*, 2021, 1–15.
184 B. Huang, C. Vyas, J. J. Byun, M. El-Newehy, Z. Huang and P. Bártolo, *Mater. Sci. Eng., C*, 2020, **108**, 110374.
185 P. Bahrami Miyanji, D. Semnani, A. Hossein Ravandi, S. Karbasi, A. Fakhrali and S. Mohammadi, *Polym. Adv. Technol.*, 2022, **33**, 81–95.
186 H. Akbari-Aghdam, A. Bagherifard, M. Motififard, J. Parvizi, E. Sheikhbahaei, S. Esmaeili, S. Saber-Samandari and A. Khandan, *Arch. Bone Jt. Surg.*, 2021, **9**, 445.
187 T. Hu, M. Shi, X. Zhao, Y. Liang, L. Bi, Z. Zhang, S. Liu, B. Chen, X. Duan and B. Guo, *J. Chem. Eng.*, 2022, **428**, 131017.
188 T. C. Suh, J. Twiddy, N. Mahmood, K. M. Ali, M. M. Lubna, P. D. Bradford, M. A. Daniele and J. M. Gluck, *ACS Omega*, 2022, **7**, 20006–20019.
189 F. Tondnevis, H. Keshvari and J. A. Mohandesi, *J. Biomed. Mater. Res., Part B*, 2020, **108**, 2276–2293.
190 S. Naskar, A. K. Panda, A. Jana, S. Kanagaraj and B. Basu, *J. Biomed. Mater. Res., Part B*, 2020, **108**, 2320–2343.
191 S. Mombini, J. Mohammadnejad, B. Bakhshandeh, A. Narmani, J. Nourmohammadi, S. Vahdat and S. Zirak, *Int. J. Biol. Macromol.*, 2019, **140**, 278–287.
192 P. Falamarzpour and S. R. Ghaffarian Anbaran, *J. Polym. Res.*, 2022, **29**, 1–10.
193 F. Luo, R. Li, H. Zheng, Y. Xu, L. Yang, C. Qu, G. Hong and Q. Wan, *Front. Bioeng. Biotechnol.*, 2022, **10**, 913080.
194 A. A. Mieloch, J. A. Semba and J. D. Rybka, *Int. J. Bioprint.*, 2022, **8**, 548.
195 M. Li, Q. Zhou, H. Song, Y. Lu, M. Lu, X. Lu, K. Duan and J. Weng, *Mater. Lett.*, 2022, **314**, 131780.
196 Q. Li, C. Yue, T. Chen, C. Ding and H. Zhang, *AIP Adv.*, 2022, **12**, 055124.
197 M. Parvizifard and S. Karbasi, *Int. J. Biol. Macromol.*, 2020, **152**, 645–662.
198 M. Masoumi, M. Jahanshahi, M. G. Ahangari and G. N. Darzi, *Appl. Surf. Sci.*, 2021, **546**, 148894.
199 A. A. Al-Allaq, J. S. Kashan, M. T. El-Wakad and A. M. Soliman, *J. Ceram. Process. Res.*, 2021, **22**, 446–454.
200 L. Sukhodub, L. Sukhodub, M. Kumeda, Y. I. Prylutskyy, M. Pogorielov, M. Evstigneev, V. Kostjukov, N. Strutynska, L. Vovchenko and S. Khrapatiy, *Prog. Biomater.*, 2020, **9**, 1–14.
201 J. Zhang, L. Zeng, Z. Qiao, J. Wang, X. Jiang, Y. S. Zhang and H. Yang, *ACS Appl. Mater. Interfaces*, 2020, **12**, 30247–30258.
202 B. Huang, C. Vyas, I. Roberts, Q.-A. Poutrel, W.-H. Chiang, J. J. Blaker, Z. Huang and P. Bártolo, *Mater. Sci. Eng., C*, 2019, **98**, 266–278.
203 E. M. Steel, J.-Y. Azar and H. G. Sundararaghavan, *Materialia*, 2020, **9**, 100581.
204 L. Liu, B. Yang, L.-Q. Wang, J.-P. Huang, W.-Y. Chen, Q. Ban, Y. Zhang, R. You, L. Yin and Y.-Q. Guan, *J. Mater. Chem. B*, 2020, **8**, 558–567.
205 C. D. Grande Tovar, J. I. Castro, C. H. Valencia, D. P. Navia Porras, J. Herminsul Mina Hernandez, M. E. Valencia Zapata and M. N. Chaur, *Molecules*, 2020, **25**, 1203.
206 J. J. Pavón, D. López, F. Mondragón, J. Gallego, S. L. Arias, K. Luitjohan, B. Holybee, Y. Torres, J. A. Rodríguez and M. Echeverry-Rendón, *J. Biomed. Mater. Res., Part A*, 2019, **107**, 719–731.
207 M. H. Mirmusavi, P. Zadehnajar, D. Semnani, S. Karbasi, F. Fekrat and F. Heidari, *Int. J. Biol. Macromol.*, 2019, **132**, 822–835.
208 A. Dominguez-Alfaro, N. Alegret, B. Arnaiz, J. M. González-Domínguez, A. Martin-Pacheco, U. Cossío, L. Porcarelli, S. Bosi, E. Vázquez and D. Mecerreyes, *ACS Biomater. Sci. Eng.*, 2019, **6**, 1269–1278.
209 M. Zarei, N. Tanideh, S. Zare, F. Sari Aslani, O. Koohi-Hosseinabadi, R. Muthuraj, I. Jamhiri, A. Rowshanghias and P. Mehryar, *J. Bioact. Compat. Polym.*, 2019, **34**, 386–400.
210 S. Saber-Samandari, M. Mohammadi-Aghdam and S. Saber-Samandari, *Int. J. Biol. Macromol.*, 2019, **138**, 810–818.
211 X. Liu, M. Chang, B. He, L. Meng, X. Wang, R. Sun, J. Ren and F. Kong, *J. Compos. Sci.*, 2019, **538**, 507–518.
212 A. M. Deliormanlı and H. Atmaca, *Int. J. Polym. Mater. Polym. Biomater.*, 2019, **68**, 1154–1166.
213 A. Shafiee, M. Kehtari, Z. Zarei, M. Soleimani, R. Varshochian, A. Ahmadi, F. Atyabi and R. Dinarvand, *Mater. Sci. Eng., C*, 2021, **120**, 111739.
214 W. Wang, B. Huang, J. J. Byun and P. Bártolo, *J. Mech. Behav. Biomed. Mater.*, 2019, **93**, 52–60.
215 S. Shrestha, B. K. Shrestha, J. Lee, O. K. Joong, B.-S. Kim, C. H. Park and C. S. Kim, *Mater. Sci. Eng., C*, 2019, **102**, 511–523.
216 S. Zhang, H. Liu, J. Gou, J. Ying, Y. Wang, C. Liu and C. Shen, *Polym. Test.*, 2019, **77**, 105904.
217 Z. Deng, T. Hu, Q. Lei, J. He, P. X. Ma and B. Guo, *ACS Appl. Mater. Interfaces*, 2019, **11**, 6796–6808.
218 C. D. Grande Tovar, J. I. Castro, C. H. Valencia, D. P. Navia Porras, J. H. Mina Hernandez, M. E. Valencia, J. D. Velasquez and M. N. Chaur, *Biomolecules*, 2019, **9**, 684.
219 J. Cao, Y. Lu, H. Chen, L. Zhang and C. Xiong, *Int. J. Polym. Mater. Polym. Biomater.*, 2019, **68**, 433–441.
220 P. Makvandi, M. Ashrafizadeh, M. Ghomi, M. Najafi, H. H. S. Hossein, A. Zarrabi, V. Mattoli and R. S. Varma, *Prog. Biomater.*, 2021, **10**, 77–89.
221 M. Mehdikhani and S. Ghaziof, *Appl. Phys. A*, 2018, **124**, 1–15.
222 F. Pouladzadeh, A. A. Katbab, N. Haghighipour and E. Kashi, *Eur. Polym. J.*, 2018, **105**, 286–296.

223 Z. Deng, Y. Guo, X. Zhao, P. X. Ma and B. Guo, *Chem. Mater.*, 2018, **30**, 1729–1742.
224 M. H. Mirmusavi, S. Karbasi, D. Semnani, M. Rafienia and A. Zargar Kharazi, *Micro Nano Lett.*, 2018, **13**, 829–834.
225 W. Pan, X. Xiao, J. Li, S. Deng, Q. Shan, Y. Yue, Y. Tian, N. R. Nabar, M. Wang and L. Hao, *J. Mater. Sci.: Mater. Med.*, 2018, **29**, 1–14.
226 S. Sharmeen, A. M. Rahman, M. M. Lubna, K. S. Salem, R. Islam and M. A. Khan, *Bioact. Mater.*, 2018, **3**, 236–244.
227 A. A. Al-allaq, J. S. Kashan, M. T. El-Wakad and A. M. Soliman, *Period. Eng. Nat. Sci.*, 2021, **9**, 930–939.
228 J. Xu, X. Hu, S. Jiang, Y. Wang, R. Parungao, S. Zheng, Y. Nie, T. Liu and K. Song, *Polymers*, 2019, **11**, 230.
229 A. G. Sanchez, E. Prokhorov, G. Luna-Barcenas, J. Hernández-Vargas, R. Román-Doval, S. Mendoza and H. Rojas-Chávez, *Mater. Today Commun.*, 2021, **28**, 102615.
230 W. Lan, X. Zhang, M. Xu, L. Zhao, D. Huang, X. Wei and W. Chen, *RSC Adv.*, 2019, **9**, 38998–39010.
231 H. Yang, J. Li, Q. Liao, H. Guo, H. Chen, Y. Zhu, M. Cai and H. Lv, *J. Mater. Res. Technol.*, 2019, **34**, 532–544.
232 A. S. Mesgar, Z. Mohammadi and S. Khosrovan, *Int. J. Polym. Mater. Polym. Biomater.*, 2018, **67**, 267–276.
233 R. Zhang, X. Li, M. Yang, X. Gao, T. Zhu and L. Lu, *J. Hard Tissue Biol.*, 2019, **28**, 217–224.
234 F. Tondnevis, H. Keshvari and J. A. Mohandesi, *J. Polym. Res.*, 2019, **26**, 1–16.
235 A. Kausar, *J. Plast. Film Sheeting*, 2021, **37**, 70–92.
236 C. M. Das, L. Kang, G. Yang, D. Tian and K.-T. Yong, *J. Compos. Sci.*, 2020, **4**, 117.
237 M. Nikbakht, S. Karbasi, S. M. Rezayat, S. Tavakol and E. Sharifi, *Polym.-Plast. Technol. Mater.*, 2019, **58**, 2031–2040.
238 T. D. Stocco, E. Antonioli, M. L. Romagnolli, G. F. Sousa, M. Ferretti and A. O. Lobo, *Mater. Lett.*, 2020, **264**, 127351.
239 R. Vasita and D. S. Katti, *Int. J. Nanomed.*, 2006, **1**, 15–30.
240 X. Han, D. Yang, C. Yang, S. Spintzyk, L. Scheideler, P. Li, D. Li, J. Geis-Gerstorfer and F. Rupp, *J. Clin. Med.*, 2019, **8**, 240.
241 C. Liao, Y. Li and S. C. Tjong, *Polymers*, 2020, **12**, 2858.
242 M. Uddin, P. S. Dhanasekaran and R. Asmatulu, *Prog. Biomater.*, 2019, **8**, 211–221.
243 D. Naskar, A. K. Ghosh, M. Mandal, P. Das, S. K. Nandi and S. C. Kundu, *Biomaterials*, 2017, **136**, 67–85.
244 G. P. Awasthi, V. K. Kaliannagounder, J. Park, B. Maharjan, M. Shin, C. Yu, C. H. Park and C. S. Kim, *Colloids Surf., A*, 2021, **622**, 126584.
245 A. Abdal-hay, M. Taha, H. M. Mousa, M. Bartnikowski, M. L. Hassan, M. Dewidar and S. Ivanovski, *Ceram. Int.*, 2019, **45**, 15736–15740.
246 P. R. Schmitt, K. D. Dwyer and K. L. Coulombe, *ACS Appl. Bio Mater.*, 2022, **5**, 2461–2480.
247 A. Savchenko, R. T. Yin, D. Kireev, I. R. Efimov and E. Molokanova, *Front. Bioeng. Biotechnol.*, 2021, **9**, 797340.
248 H. Öztatlı and D. Ege, *MRS Adv.*, 2017, **2**, 1291–1296.
249 L. Roseti and B. Grigolo, *J. Exp. Orthop.*, 2022, **9**, 1–7.
250 N. S. Golshayan, S. Karbasi, E. Masaeli, E. Bahremandi-Toloue, M. H. Nasr-Esfahani and M. Rafienia, *Polym.-Plast. Technol. Mater.*, 2022, **61**, 1244–1264.
251 Z. Deng, H. Han, J. Yang, Y. Li, S. Du and J. Ma, *Med. Sci. Monit.*, 2017, **23**, 2479.
252 H. Zhang, L. Lin, L. Ren, Y. Liu and R. Song, *J. Appl. Polym. Sci.*, 2021, **138**, 50166.
253 C. Grabinski, S. Hussain, K. Lafdi, L. Braydich-Stolle and J. Schlager, *Carbon*, 2007, **45**, 2828–2835.
254 J. S. Czarnecki, K. Lafdi, R. M. Joseph and P. A. Tsonis, *Tissue Eng., Part A*, 2012, **18**, 946–956.
255 Y. Han, Y. Lv, J. Chen, M. Yao, C. Wang, P. Hu and Y. Liu, *ACS Appl. Polym. Mater.*, 2021, **3**, 4195–4202.
256 P. Zadehnajar, B. Akbari, S. Karbasi and M. H. Mirmusavi, *Int. J. Polym. Mater. Polym. Biomater.*, 2020, **69**, 326–337.
257 P. Zadehnajar, S. Karbasi, B. Akbari and L. Ghasemi, *Mater. Technol.*, 2020, **35**, 39–49.
258 J. S. L. Fong, M. A. Booth, A. Rifai, K. Fox and A. Gelmi, *Adv. Healthcare Mater.*, 2021, **10**, e2100007.
259 L. Bacakova, J. Pajorova, M. Tomkova, R. Matejka, A. Broz, J. Stepanovska, S. Prazak, A. Skogberg, S. Siljander and P. Kallio, *Nanomaterials*, 2020, **10**, 196.
260 Q. Zhang, V. N. Mochalin, I. Neitzel, I. Y. Knoke, J. Han, C. A. Klug, J. G. Zhou, P. I. Lelkes and Y. Gogotsi, *Biomaterials*, 2011, **32**, 87–94.
261 Y. Sun, A. Finne-Wistrand, T. Waag, Z. Xing, M. Yassin, A. Yamamoto, K. Mustafa, D. Steinmüller-Nethl, A. Krueger and A.-C. Albertsson, *Macromol. Mater. Eng.*, 2015, **300**, 436–447.
262 D. Karaman and H. Ghahramanzadeh Asl, *Proc. Inst. Mech. Eng., Part H*, 2022, **236**, 794–810.
263 A. Timercan, V. Sheremetyev and V. Brailovski, *Sci. Technol. Adv. Mater.*, 2021, **22**, 285–300.
264 Y. C. Chen, D. C. Lee, N. H. Tai and I. M. Chiu, *Diamond-Based Materials for Biomedical Applications*, 2013, pp. 171–185.
265 J. Liskova, O. Babchenko, M. Varga, A. Kromka, D. Hadraba, Z. Svindrych, Z. Burdikova and L. Bacakova, *Int. J. Nanomed.*, 2015, **10**, 869–884.
266 P. B. Milan, S. Khamseh, P. Zarrintaj, B. Ramezanzadeh, M. Badawi, S. Morisset, H. Vahabi, M. R. Saeb and M. Mozafari, *Heliyon*, 2020, **6**, e03798.
267 R. Aversa, R. V. V. Petrescu, A. Apicella and F. I. T. Petrescu, *Eng. Rev.*, 2019, **39**, 81–89.
268 R. Aversa, R. V. V. Petrescu, A. Apicella and F. I. T. Petrescu, *Am. J. Biochem. Biotechnol.*, 2017, **13**, 34–41.
269 M. Mahdavi, N. Mahmoudi, F. Rezaie Anaran and A. Simchi, *Mar. Drugs*, 2016, **14**, 128.
270 L. Yate, L. E. Coy, D. Gregurec, W. Aperador, S. E. Moya and G. Wang, *ACS Appl. Mater. Interfaces*, 2015, **7**, 6351–6358.
271 C. Shuai, W. Huang, P. Feng, C. Gao, D. Gao, Y. Deng, Q. Wang, P. Wu and X. Guo, *J. Porous Mater.*, 2016, **24**, 249–255.
272 C. D. Grande Tovar, J. I. Castro, C. H. Valencia, D. P. Navia Porras, J. H. Mina Hernandez, M. E. Valencia, J. D. Velasquez and M. N. Chaur, *Biomolecules*, 2019, **9**, 684.

273 M. Vedhanayagam, B. U. Nair and K. J. Sreeram, *Materialia*, 2019, **7**, 100354.
274 A. Kausar, *J. Plast. Film Sheeting*, 2020, **36**, 409–429.
275 D. Kai, M. J. Tan, M. P. Prabhakaran, B. Q. Y. Chan, S. S. Liow, S. Ramakrishna and X. J. Loh, *Colloids Surf., B*, 2016, **148**, 557–565.
276 M. K. Haider, L. Sun, A. Ullah, S. Ullah, Y. Suzuki, S. Park, Y. Kato, Y. Tamada and I. S. Kim, *Mater. Today Commun.*, 2021, **27**, 102259.
277 S. Yousefiasl, M. Imani, I. Zare, S. Samaei, R. E. Ashtiani and E. Sharifi, *Electrically Conducting Polymers and Their Composites for Tissue Engineering*, 2023, pp. 109–136.
278 T. Kaur and A. Thirugnanam, *J. Mater. Sci. Technol.*, 2017, **33**, 734–743.
279 N. C. Jeremy Kong Yoong Lee, S. Peng, L. Li, L. Tian, N. Thakor and S. Ramakrishna, *Prog. Polym. Sci.*, 2018, **86**, 40–84.
280 M. Vedhanayagam, I. S. Raja, A. Molkenova, T. S. Atabaev, K. J. Sreeram and D. W. Han, *Int. J. Mol. Sci.*, 2021, **22**, 5378.
281 Z. Peng, T. Zhao, Y. Zhou, S. Li, J. Li and R. M. Leblanc, *Adv. Healthcare Mater.*, 2020, **9**, e1901495.
282 S. Gogoi, M. Kumar, B. B. Mandal and N. Karak, *RSC Adv.*, 2016, **6**, 26066–26076.
283 S. K. Kailasa, D. J. Joshi, M. R. Kateshiya, J. R. Koduru and N. I. Malek, *Mater. Today Chem.*, 2022, **23**, 100746.
284 Y. Wang, Y. Xue, J. Wang, Y. Zhu, Y. Zhu, X. Zhang, J. Liao, X. Li, X. Wu, Y. X. Qin and W. Chen, *Polymers*, 2019, **11**, 1112.
285 M. Ghanbari, M. Salavati-Niasari and F. Mohandes, *RSC Adv.*, 2021, **11**, 18423–18431.
286 S. Rastegar, M. Mehdikhani, A. Bigham, E. Poorazizi and M. Rafienia, *Mater. Chem. Phys.*, 2021, **266**, 124543.
287 A. Vedadghavami, F. Minooei, M. H. Mohammadi, S. Khetani, A. R. Kolahchi, S. Mashayekhan and A. Sanati-Nezhad, *Acta Biomater.*, 2017, **62**, 42–63.
288 K. Ghosh, Z. Pan, E. Guan, S. Ge, Y. Liu, T. Nakamura, X.-D. Ren, M. Rafailovich and R. A. Clark, *Biomaterials*, 2007, **28**, 671–679.
289 G. Lalwani, A. Gopalan, M. D'Agati, J. Srinivas Sankaran, S. Judex, Y. X. Qin and B. Sitharaman, *J. Biomed. Mater. Res., Part A*, 2015, **103**, 3212–3225.
290 T. D. Nguyen, O. E. Kadri, V. I. Sikavitsas and R. S. Voronov, *Appl. Sci.*, 2019, **9**, 2381.
291 M. Porwal, V. Rastogi and A. Kumar, *MOJ Bioequiv. Bioavailab.*, 2017, **3**, 114–116.
292 J. V. Veetil and K. Ye, *Biotechnol. Prog.*, 2009, **25**, 709–721.
293 M. Alavi, E. Jabari and E. Jabbari, *Expert Rev. Anti-Infect. Ther.*, 2021, **19**, 35–44.
294 H. Mohammaddokht, S. M. Mahdizadeh, E. Khodeir, M. Baniadam, J. Sargolzaei, M. Maghrebi, M. E. Karkhanechin, M. Mokhtarifar and H. Arab, *Mater. Res. Express*, 2019, **6**, 095010.
295 A. Thakor, J. Jokerst, C. Zavaleta, T. Massoud and S. Gambhir, *Nano Lett.*, 2011, **11**, 4029–4036.